SESSION 6

INSTRUMENTS AND SAMPLING

Tuesday: August 25, 1992
Co-Chairmen: D. W. Moeller
W. R. A. Goossens

DIRECT POST-ACCIDENT SAMPLING SYSTEM FOR CONTAINMENT ATMOSPHERES (DI-PAS SYSTEM)

Bernd Eckardt
Siemens AG, Power Generation Group (KWU)
W-6050 Offenbach am Main
Federal Republic of Germany

Abstract

In order to reduce the residual risk associated with hypothetical severe nuclear accidents, nuclear power plants in Germany have been backfitted amongst other things with supplementary systems such as containment venting systems[1][2]. In conjunction with these measures the German Reactor Safety Commission (RSK) imposed the additional requirement that provisions be made for representative post-accident sampling of the containment atmosphere for the purpose of obtaining information on the condition of the core and on potential hazards to the environment.

To meet this requirement, enveloping conditions for relevant accident scenarios were defined, such as an enveloping aerosol with an aerodynamic diameter in the range of 0.1 to 10 µm, widely varying iodine concentrations, and humidity, pressure and temperature conditions. In addition to these basic requirements it is also considered appropriate to provided a possibility for measurement of the gas composition, e.g. CO, CO_2, H_2 and O_2.

An investigation of the existing options for piping system sampling with pipe lengths of up to 50 m based on this requirement revealed that, despite the use of special piping materials and heat tracing equipment, etc. considerably high pipe factors for iodine and aerosols as well as significant memory effects would have to be expected under the various accident conditions in question, including impurity effects.

Consequently, new sampling systems based on sample transport via piping systems and sample collection outside the containment, as well as systems for direct post-accident sampling inside the containment (Di-PAS systems) were designed and the characteristics of the two approaches compared.

The results of this comparison clearly favored the use of Di-PAS systems with in-situ samplers which could, for example, be pneumatically transported into the containment to perform sampling (pneumatic conveyor principle) and other direct-type sampling systems.

Finally, in order to minimize cost and effort and to provide exclusively passive components inside the containment, an in-situ scrubber sampling unit was developed. The German nuclear plant owners and operators commissioned tests of this unit to verify its

suitability for sample transport over distances in excess of 50 meters.

The main result of these tests is that pipe factors for substances capable of deposition could be almost completely eliminated despite sample transport over 30 - 50 meters, meaning that representative sampling is possible even under such extreme conditions.

In addition, the system presented herein is designed such that it can, if required, also be used to extract and appropriately condition water samples using the equipment already available in the system.

1. Introduction

The requirement for a sampling system providing representative samples even under severe accident conditions must be seen in the light of the particular significance of containment atmosphere activities as regards the environment.

In order to determine system requirements, various enveloping hypothetical accident situations were analyzed together with German plant owners and operators and the most important enveloping system requirements were formulated.

Measurement of the composition of the containment atmosphere is intended to allow assessment of the potential hazard for the area around the plant as well as providing additional information on the accident history, the plant condition and the effect of countermeasures. For this reason the airborne radionuclide concentrations are of particular interest as well as measurement of the gas composition, e.g. for CO, CO_2, H_2 and O_2. Depending on the accident sequence the postulated accident conditions can result in considerably higher concentration levels as compared to a design basis accident (DBA).

The following describes the functions of existing and newly-developed systems:

- specially for the in-situ pool sampler system
- for measurement of airborne nuclide concentrations as the main task as well as for additional functions such as gas concentration sampling (CO, CO_2, H_2 and O_2, etc.) and water sampling.

2. System Functional Requirements

The function of the sampling system is to extract a representative sample from the containment atmosphere which would provide information helpful in assessing the accident sequence, the plant condition and the potential hazard to the environment.

Functional Requirements

The following nuclides have to be detected:

- concentration of aerosol-bound radionuclides
- concentration of gaseous iodine and iodine compounds
- concentration of other substances present in gaseous form (noble gases).

Further important requirements include:

- cross-contamination of one sample to another through "memory effects" or prior contamination during transient accident phases should be avoided as far as possible
- measurement of other components of the atmosphere such as H_2, O_2, CO, CO_2 should also be possible.

Determination of the CO/CO_2 concentration, for example, can provide information on whether there has been a significant increase in the natural CO_2 portion of the containment atmosphere of < 0.03 vol%, or in the hydrogen and oxygen concentrations during an accident. The possibility to perform such analyses is, for example, also required by the Gesellschaft für Reaktorsicherheit (GRS)[11].

In addition the system concept shall have the potential possibility of:

- sampling water, e.g. from the sump or other water-containing sysems, as well as measuring water levels.

Further relevant conditions to be taken into account are as follows:

Thermodynamic Conditions

The thermodynamic conditions should cover hypothetical accident sequences which vary for PWR and BWR plants and were formulated as follows:

Containment pressure/temperature	1-7 bar/50-160 °C
Conditions	saturated and dry atmospheres

Particle Sizes

On the basis of DEMONA and VANAM measurements[7][8] and NAUA calculations[9][10], depending on physical sampling conditions and on the time of sample extraction, aerosol particles having aerodynamic diameters (d_{ae}) in the range of 0.1 to 10 µm are to be expected to occur at the place of sample extraction. Furthermore in phases with fog in the atmosphere, contaminated vapor droplets of up to approximately 30 µm must be expected. As a consequence an enveloping aerosol spectrum depending on accident scenario and time of measurement with relevant aerosol portions would cover the following diameters:

Aerosols	d_{ae}	0.1 - 10 µm
Fog	d	≤ 30 µm
Iodine	gaseous	

Activity Concentration

The system should be designed such that the first sample can already be taken 3 hours after onset of the accident (end of chain reaction). This results in the following concentrations in the containment which were used in system design:

Maximum concentration in containment during sampling		Sample activity after dilution
Noble gases	$2.7*10^{15}$ Bq/m^3	
Aerosols	$5*10^{15}$ Bq/m^3	< 10^9 Bq
Elemental iodine	$4.5*10^{15}$ Bq/m^3	
Organic iodine	$4.5*10^{15}$ Bq/m^3	

Measurements should also be performed for an extended period following accidents, where activities are significantly reduced, while avoiding memory effects.

Analysis

Sample analysis should be performed using routine methods used at the plant and should therefore use the gamma spectrometers available in the radiochemical laboratories of the nuclear power plants. The activity of samples for analysis should not exceed 10^9 Bq for handling reasons.

3. Sampling Systems

In order to fulfill the aforementioned requirements investigations were performed on the capability of existing sampling systems for DBA conditions to fulfill the newly-formulated requirements for severe accident conditions.

Extraction of Diluted Sample

The most important requirement concerning the layout of these systems was that the station for manual extraction of a sample for laboratory analysis should be well-shielded from the containment and arranged such as to remain accessible following a severe accident.

On the other hand the sample extraction point in the containment should be representative of the atmosphere in the entire containment and in a PWR, for example, should allow extraction from the inner containment area. This results in the requirement that the system to be selected must still allow detection of the substances mentioned even with pipe lengths for example of 30 - 50 m and more. A possible arrangement for a PWR is shown in Figure 2. For BWRs, transport lines tend to be longer with more pipe bends.

3.1 Measuring Problems with Various System Concepts

Different sampling system concepts have been assessed on the basis of existing results from tests performed on different piping systems. Investigations showed that systems with piping lengths of approximately 50 m already installed in power plants, as illustrated in Figure 1, exhibit considerable pipe factor problems particularly under certain severe accident scenarios. Deposition rates determined on the basis of various experiments[2][3][4] when extrapolated

for iodine in sampling systems with sampling line lengths of 50 m resulted in pipe factors of up to 10 and more. This already significant deposition of elemental iodine can furthermore be considerably affected by contamination in the form of organic impurities etc. within the system caused by the accident atmosphere. Another problem with such systems is posed by significant memory effects later in the accident sequence after there has been a considerable reduction in atmospheric contamination, something which - as in the case of deposition - can lead to severe falsification of measured values. Similar deposition problems with aerosols occur during particular accident situations where considerable aerosol fractions occur in the sampling lines.

Preference was therefore given to systems with in-situ sampling directly in the containment which would completely avoid the above problems.

3.2 New System Development

In this connection reference was made to experience in aerosol sampling technology[6] (shown as an example in Fig. 3) gained during the containment aerosol experiments DEMON and VANAM at Battelle in Frankfurt am Main as well as the ACE tests at Battelle Northwest in Richland, USA. In these experiments the sample filters were located and loaded directly in the containment atmosphere (see Fig. 3, Diagram A) to avoid significant deposition in sampling lines. This (as well as Fig. 3, Diagram B) allowed representative samples to be taken under considerably varying accident conditions with large fluctuations in aerosol particle size distribution, density of the atmosphere, moisture content and temperature, etc.

Based on calculations and on the knowledge gained during such experiments, various direct sampling systems, e.g. one with a pneumatic conveyor system and one with a shaft-driven conveyor system, an example of which is shown in Figure 4, were considered to represent a favorable solution. The disadvantage of such systems was the amount of equipment required as well as active components in the containment.

For this reason further direct monitoring systems using passive in-situ samplers were designed and investigated. This solution was found to be preferable and is described in the following (see also Fig. 5).

This system has been selected by the German owners and operators and recommended by them to the Reactor Safety Commission (RSK) for monitoring severe accident scenarios in addition to the equipment provided for design basis accidents.

4. In-Situ Pool Sampler System

In order to avoid significant sampling errors which can occur particularly during accidents where sampling conditions vary considerably, samples of substances likely to be deposited in sampling lines are taken directly in the containment.

4.1 Sampling of Aerosols, Iodine and Noble Gases

The sampling unit which operates with liquid collects most of the aerosols and iodine. The nobles gas and a portion of the organic iodide which do not form deposits are routed to dilution equipment outside the containment. This dilution equipment is used to extract gas and liquid samples and dilute them to an activity concentration suitable for laboratory purposes.

The main features of this system comprise:

- Separation of iodine and aerosol activities directly at the point of sample extraction by means of the pool sampler
- Operation of pool sampler under the pressure and temperature conditions prevailing in the containment
- Null sample extraction before each sampling operation
- Extraction of gas sample after separation
- Extraction of a portion of the scrubbing liquid via a piping system to a remote sampling station
- Sample extraction downstream of the dilution loops via septum and determination of the concentration of the gas sample or in the scrubbing liquid sample through laboratory analysis of the sample using routine methods
- Decontamination of the entire system following sampling measurements through flushing.

4.2 Measurement of Gas Concentration

Through operation of the system with an upstream pool, aerosols and iodine are for the most part removed from the gas sample. The pool liquid can be varied according to the gas sample required for collection. In order to allow detection of the various gas components such as CO, CO_2, H_2 and O_2 in the laboratory using gas chromatography it is necessary to perform reduced dilution of $\leq$ 1000 and less. Integration of a dilution unit for variable operation, e.g. between 1:10 and 1:1000 dilution in the system, enables gas sample dilution to values above the detection threshold of the existing laboratory measuring equipment making quantitative verification possible.

4.3 Liquid Sampling

The system can be used for multiple functions, also for extraction and conditioning of water samples, as the appropriate system functions are already available, allowing samples to be taken from the containment sump or residual heat removal systems and conditioned for example using the same basic process. This function will not be described in detail here and is not required by German plant owners and operators.

5. Verification

Thermohydraulic function, separation and deposition properties were investigated for this equipment during tests which used realistic piping lengths of 30 to 50 m. The following will briefly illustrate the particular problem of transport losses in sampling equipment and transport lines, as well as memory effects, on the basis of test results.

5.1 Loss Factors for Liquid Transport

Falsification of measured values is also possible during liquid transport as a result of the following:

- Suspended particles are deposited during transport (reduction in concentration)
- A portion of the scrubbing liquid from the previous filling procedure remains in the line and dilutes the sample subsequently extracted.

The amount remaining in the line is roughly known but remains for the most part non-contaminated. Subsequent mixing with the contaminated scrubbing liquid therefore also results in reduction of the concentration. This effect has been minimized in the course of system testing and development.

The loss factor which is influenced by both these effects was determined in the test facility by measuring the concentration of the scrubber fluid both directly at the sampler and in the suitably-extracted fraction at the end of the sampling line. These loss factors were determined both for a soluble substance (potassium iodide) as well as for a suspended substance (barium sulfate aerosol). The substances were introduced into the inlet area of the in-situ sampler in solution or suspension, in part as wall contamination. Following decontamination and transport processes the concentration was determined. The results of some of these tests are shown in Figure 7 so that sampling losses can be minimized and pipe factors of < 1.5 can be obtained.

5.2 Memory Effects

Falsification of the results of measurements for substances capable of separation could also possibly occur as a result of scrubbing liquid residue or contaminants in the pool sampler originating from previous measurements or, when the system is not in operation, directly from the containment atmosphere. These become particularly significant in the event of further measurements during an extended period following an accident, if concentrations are considerably lower.

In order in this case to retain the required measurement accuracy the entire system equipment can be decontaminated and a null sample be taken to determine the background contamination. The time function for system decontamination is shown in Appendix 10. After a short flushing period, the concentration is less than 1% of the original concentration.

5.3 Results

The tests described here, as well as additional more recent tests, allow confirmation of the following for the sampling equipment:

- For most part representative sampling for enveloping aerosol spectrum and elemental iodine through in-situ sampling

- For most part avoidance of pipe factor problems through
  - consideration also of deposits at sampling equipment inlet area
  - transport in liquid of substances likely to deposit
  - regular flushing of suction inlet

- Insignificant memory effects through
  - null sample before the start of measurement and
  - system flushing (decontamination) after measurement/fouling

- Operation of equipment from well-shielded area possible e.g. via sampling line of 50 m or more

- Fully remote-controlled operation of the passive in-situ sampler unit

- $H_2/O_2/CO/CO_2$ measurement in sampling gas atmosphere with reduced dilution factors of ≤ 1000 possible.

References

1 Eckardt, B.A.
"Sliding pressure venting process for BWRs and PWRs"
IAEA Meeting, Stockholm, 10 - 13/09/1991

2 Heck, R.
"Concept and qualification of a combined system for hydrogen mitigation after severe accidents"
Toronto, October 14 - 17, 1990

3 Wright, A.L., Fish, B R., Beahm, E.C., Weber, C.F.
"The chemistry and behavior of iodine-vapor species in nuclear plant air-monitoring sampling lines"
Oak Ridge National Laboratory, Oak Ridge, Tennessee 37831
20th DOE/NRC Nuclear Air Cleaning Conference

4 Unrein, P.G., Pelletier, C.A., Cline, J.E., Voillequé, P.G.
"Transmission of radioiodine through sampling lines"
Science Applications, Inc., Rockville, Maryland 20850
18th DOE Nuclear Airborne Waste Management and Air Cleaning Conference

5 Kabat, M.J.
"Deposition of airborne radioiodine species on surfaces of metals and plastics"
Ontario Hydro Health and Safety Division
17th DOE Nuclear Air Cleaning Conference

6 Kanzleiter, T., Valencia, L.
"Instrumentation used for containment experiments under severe accident conditions"
Battelle-Institut e.V., Frankfurt am Main

7 DEMONA
Annual Report 1985 (in German only)
KfK 4182

8 Kanzleiter, T.
"VANAM multi-compartment aerosol depletion experiment M2"
Technical Report BIeV-R67.098-302, February 1991

9 Bünz, H., Koyro, M., Schöck, W.
"NAUA Calculations" NAUA Mod 5 and NAUA Mod 5-M (in German only) KfK 4278, September 1987

10 Bunz et al.
"Mass and particle size distribution of aerosol in the pressure relief phase of a core melt accident in a PWR" (in German only)
Kernforschungszentrum Karlsruhe, June 12, 1989

11 Sonnenkalb, M., Tiltmann, M.
"Information and requirements needed for accident mitigation"
Gesellschaft für Reaktorsicherheit (GRS) mbH, Cologne,
March 16-17, 1992

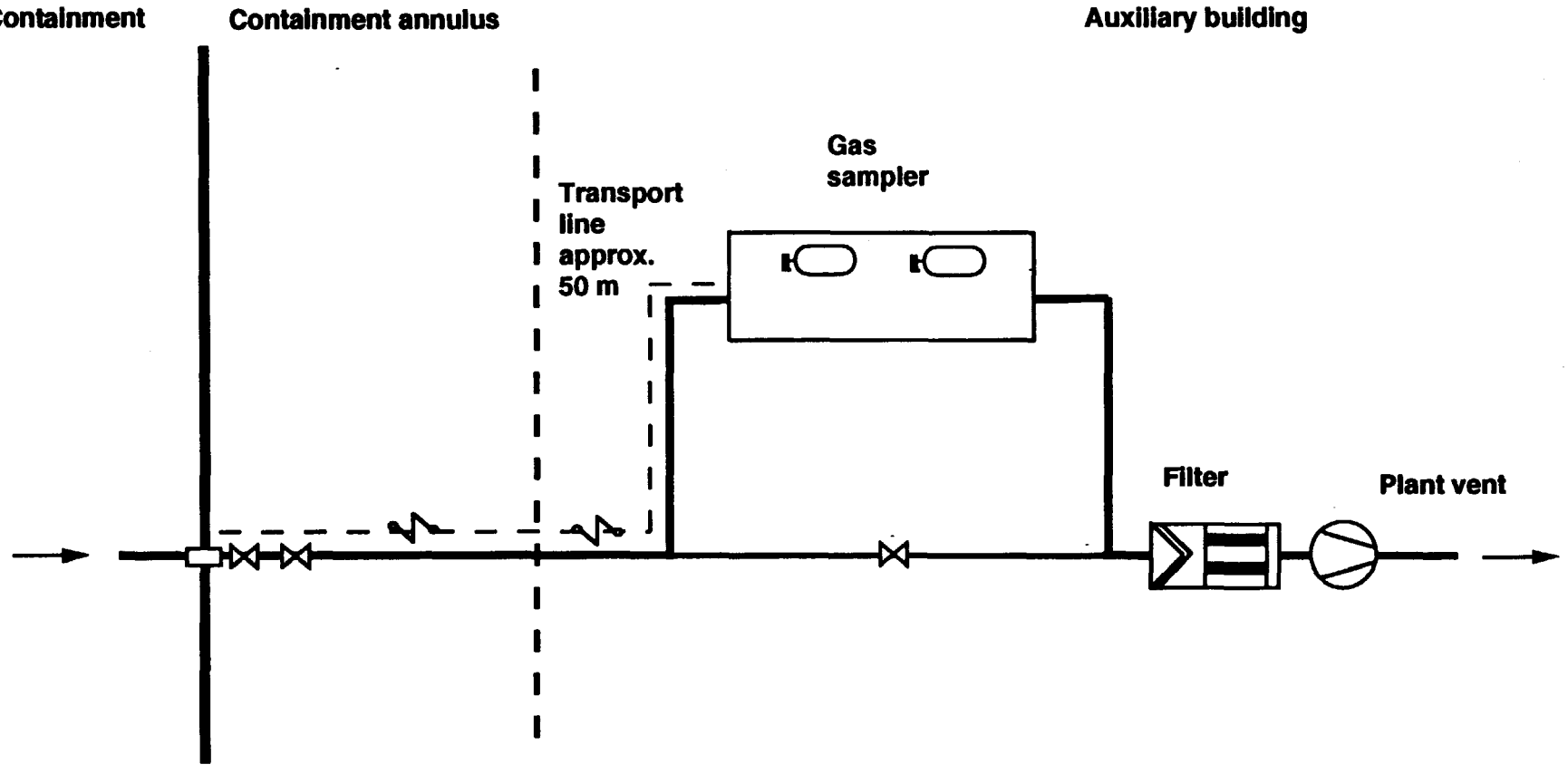

Figure 1 Existing DBA atmosphere sampling system

S/KWU
Et/06.92
09-46-G

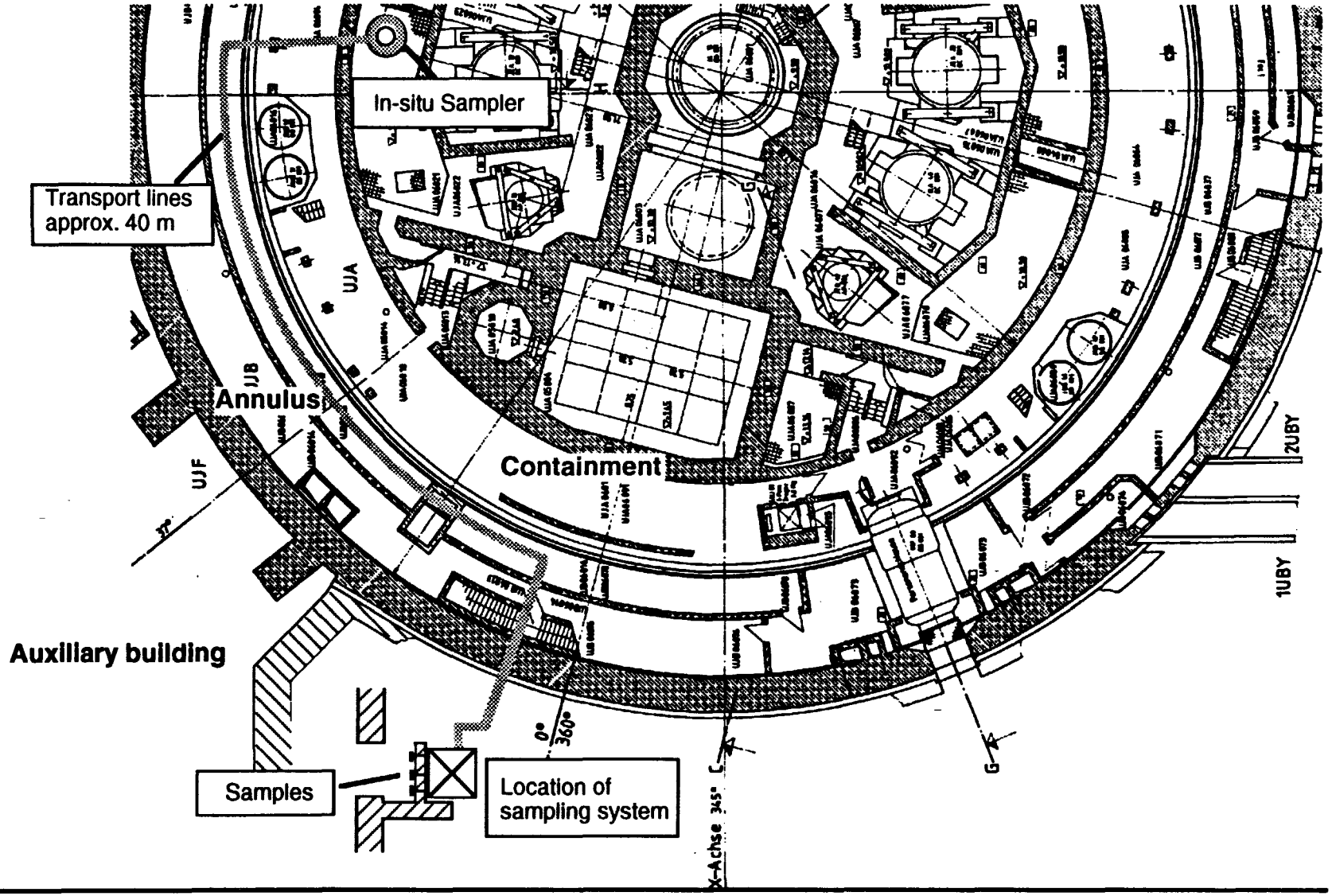

Figure 2 Arrangement of DI-PAS System for PWR

UB KWU
E 443 12.91
50-001-J

SIEMENS

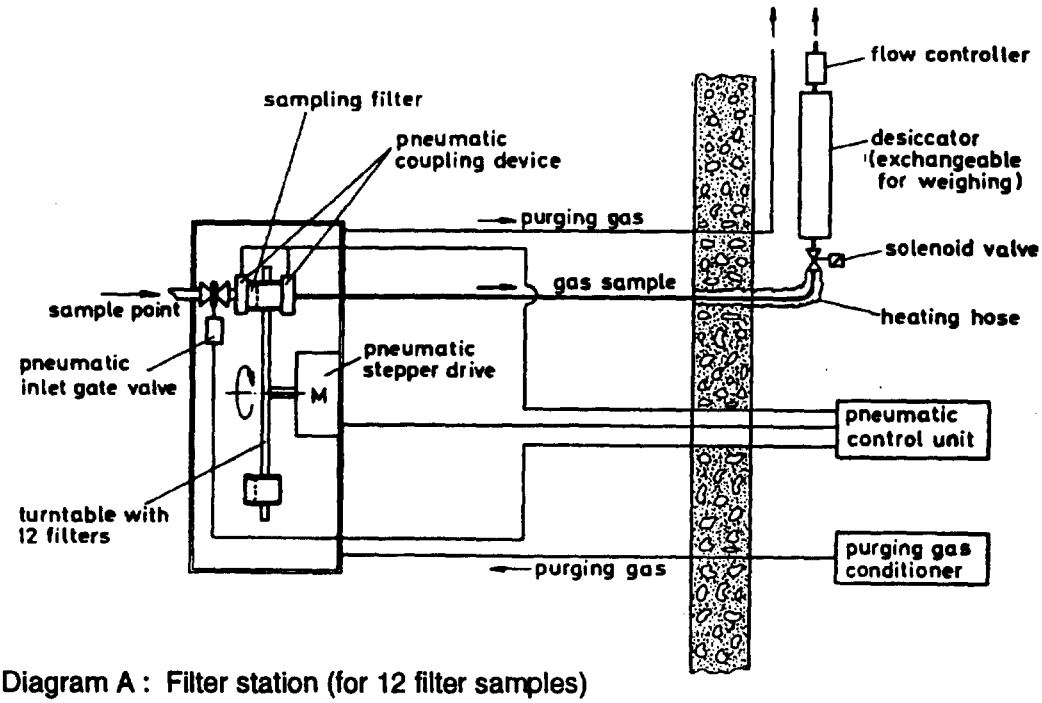

Diagram A : Filter station (for 12 filter samples)
to measure aerosol concentration, particle size and composition

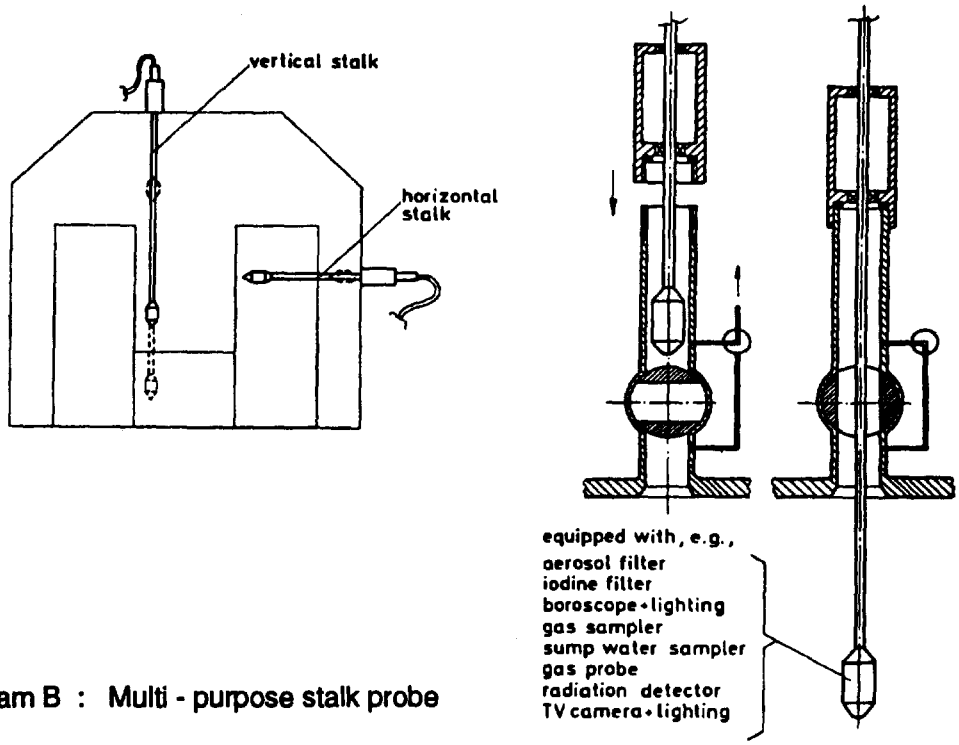

Diagram B : Multi - purpose stalk probe

Figure 3 Examples for in-situ sampler from aerosol test DEMONA/ VANAM (see Ref. 6)

S/ KWU
E443 6.92
09-001-H

SIEMENS

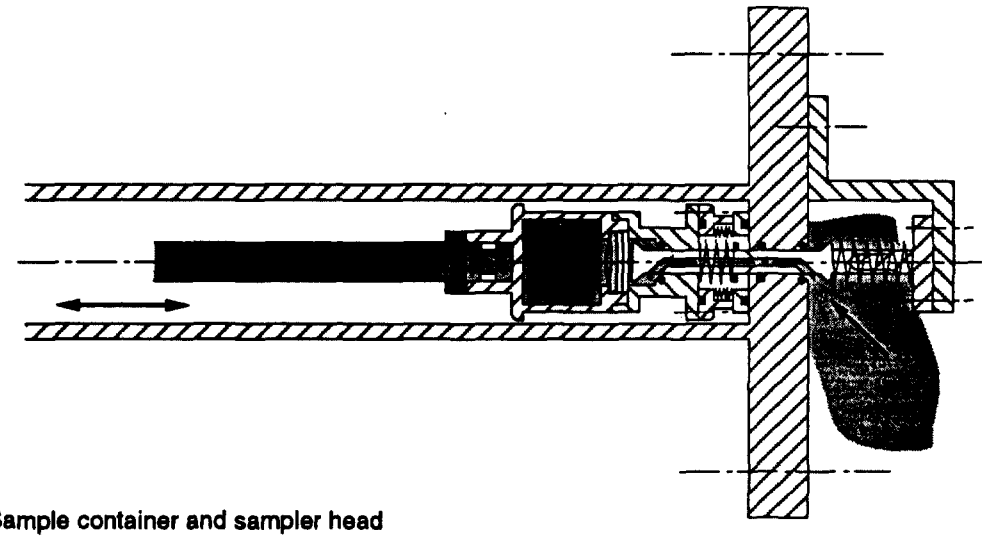

Sample container and sampler head

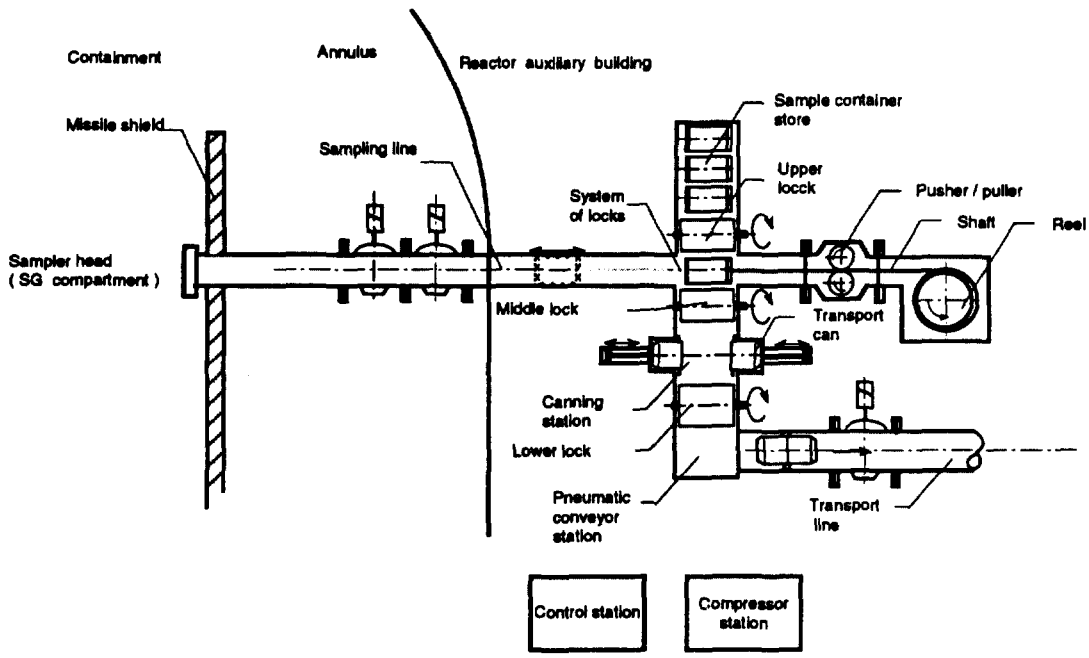

Figure 4 Example of shaft-driven conveyor system

S/KWU
E443 6.92
09-002-H

SIEMENS

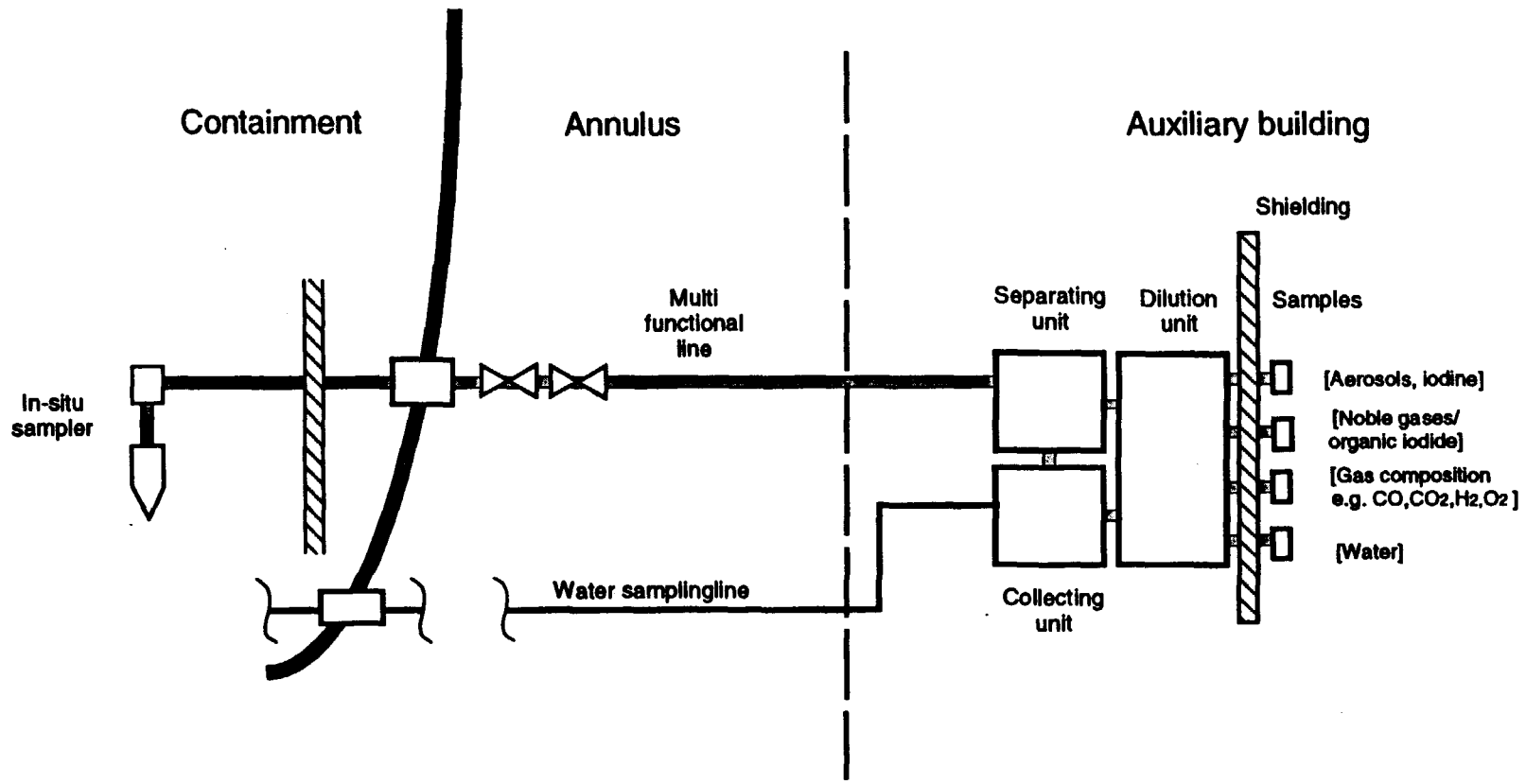

Figure 5 Schematic of Di- PAS system for PWR

S/ KWU
E 443 06.92
09-003-H

SIEMENS

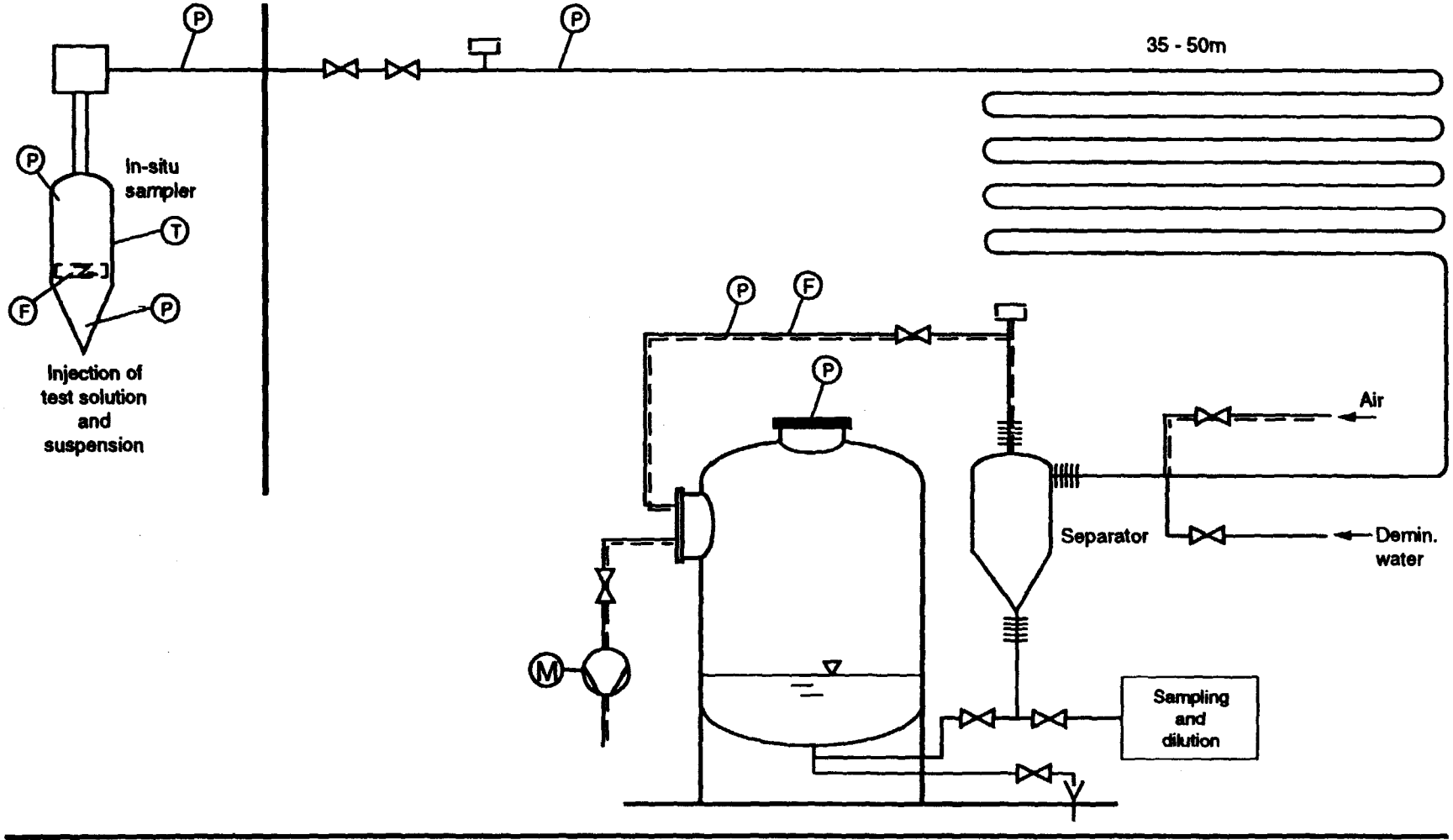

Figure 6 Test facility: Remote-controlled in-situ sampling system

S/ KWU
E443 6.92
09-004-H

SIEMENS

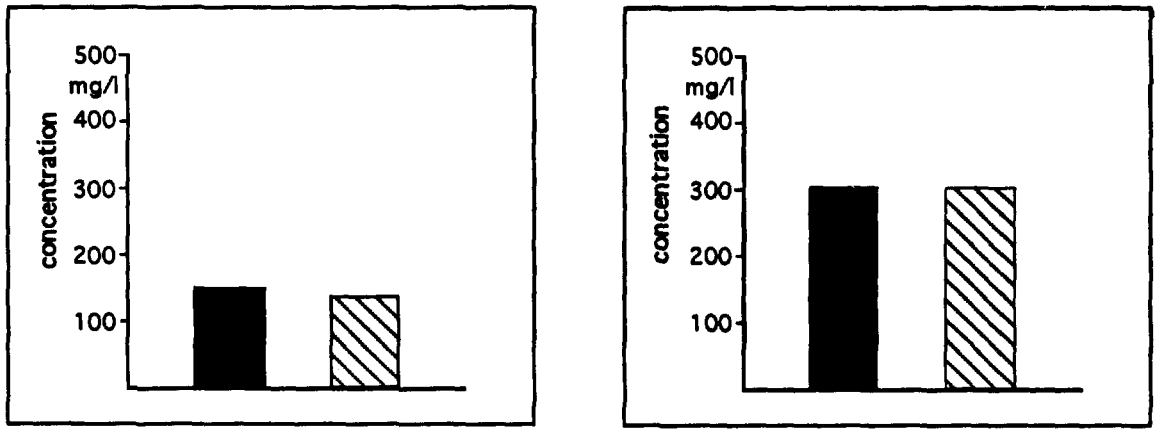

Test I potassium iodide

Loss factor R = 1.03

Test II potassium iodide

Loss factor R = 1.0

Measurement in pool

Measurement in system after transport through line of approx. 40 m

Test of system transport losses

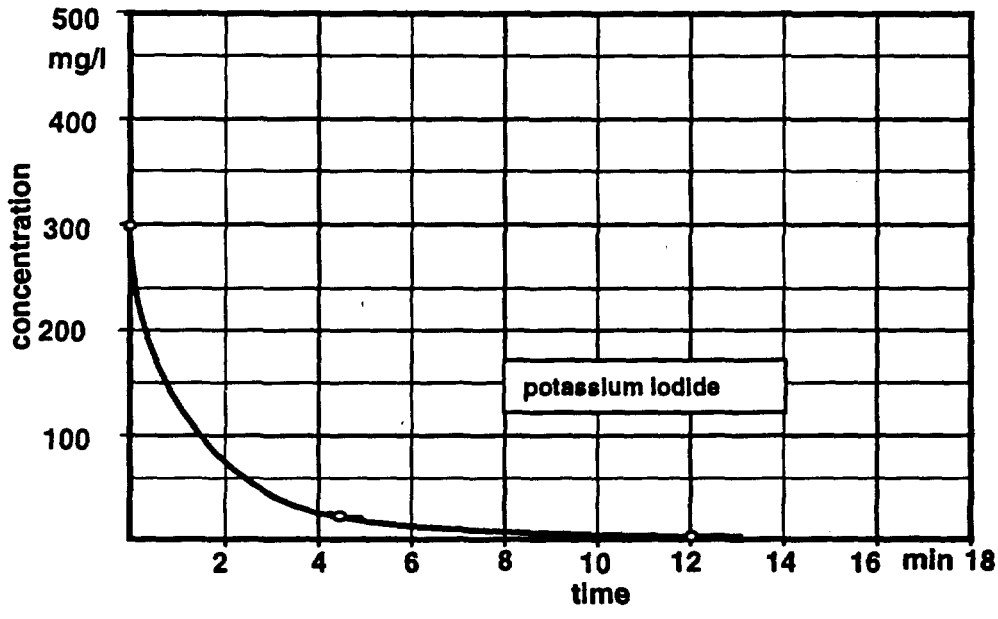

System decontamination test

Figure 7 Tests of system transport losses and decontamination

S/KWU
E443 06.92
09-005-H

PERFORMANCE CHARACTERIZATION OF A NEW CAM SYSTEM

M.J. Koskelo[1], J.C. Rodgers[2], D.C. Nelson[2],
A.R. McFarland[3] and C.A. Ortiz[3]

[1]Canberra Industries, Meriden, CT 06450
[2]Los Alamos National Laboratory, Los Alamos, NM 87545
[3]Department of Mechanical Engineering,
Texas A&M University, College Station, TX 77843

Abstract

Continuous Air Monitors (CAMs) are used in nuclear facilities to detect airborne alpha-emitting transuranic radionuclides in work areas, stacks and ducts. We have now tested the first commercial version of the original Los Alamos/Texas A&M design for its performance. The penetration of inhalable-size particles onto the CAM filter is better than 80%, with excellent uniformity of sample. With the patented diffusion screen in place, the reduction of freshly formed radon decay products is 99%.(1) With or without the diffusion screen in place, the new background compensation algorithm shows reliable detection and alarm capabilities in environments with freshly formed as well as aged radon progeny.

I. Introduction

The primary function of a Continuous Air Monitor (CAM) is to issue an alarm if the transuranic activity exceeds a preset level, so that the appropriate safety procedures may be initiated. At the same time, the alarm should not be triggered unnecessarily by the presence of the naturally occurring radon progeny. The Department of Energy (DOE) Order 5480.11(2) includes a requirement that a CAM should be able to alarm at an exposure level of 8 DAC-hours under controlled laboratory conditions. However, designing a CAM that can reliably alarm at 8 DAC-hours under field conditions has been a difficult goal to achieve.

Some CAM inlet designs have been shown to have difficulties obtaining a representative sample of the inhalable-size particles ($\leq$ 10 μm aerodynamic equivalent diameter) without significant loss or bias.(3) Some designs show significant non-uniformity of filter deposits.(3,4) If the aerosol particles are predominantly deposited near the edge of the filter, the transuranic concentration in the air will be underestimated; and if the deposits are mainly in the center of the filter, the concentration will be overestimated.(5) Also, the commonly used numerical algorithms for subtracting the counts in low energy tail of the 6 MeV radon daughter sometimes have difficulty distinguishing the transuranic counts from the radon daughter interference, if the radon level is elevated.

To address these difficulties, the Los Alamos National Laboratory, together with the Aerosol Technology Laboratory of

Texas A&M University launched an effort to develop a new generation CAM. This effort had several important goals including: obtaining a representative air sample and depositing it uniformly on the filter of the unit; partial removal of the radon daughter products from the air stream; and, an accurate background compensation algorithm. In addition, it had to reliably alarm at an exposure level of 8 DAC-hours or less with a minimum false alarm rate.

Several of the design goals were already reached during the development of the first prototype. The problems of obtaining representative air samples, removing a large fraction of the radon daughter products from the air flow and producing uniform sample deposits were resolved during that phase of the project. A description of the results obtained with the Los Alamos/Texas A&M CAM prototype have been reported elsewhere.[1,3,5,6] In this work, we report on the testing of the first commercial version developed from the original Los Alamos/Texas A&M design. In addition to repeating the tests on the penetration of inhalable-size particles onto the CAM filter and the uniformity of the sample, we have included tests to verify the alarm capabilities of the new background compensation algorithm which has been added to this commercial version.

II. Background Compensation Algorithm

To illustrate why a sophisticated background compensation algorithm is required, let us consider a typical CAM spectrum as illustrated in Figure 1. It has four distinctly separate regions which are marked as regions 0 to 4. Region 0 below channel X_0 is of no particular interest. Region 1 between channels X_0 and X_1 denotes the interval which contains all the transuranic counts. Region 2 between channels X_1 and X_2 denotes the channels for the 6.0 MeV background radiation. Region 3 between channels X_2 and X_3 denotes a region for the 7.68 MeV background peak, and Region 4 is the spectrum above X_3. However, as can be seen from Figure 1, the background peaks have pronounced tails, which extend well into Region 1 and must therefore be subtracted from it to calculate the net transuranic content in the spectrum.

To calculate these tails, we have adapted a method from a more general purpose alpha spectroscopy algorithm.[7] We first calculate the "valley" channels, X_n, based on an energy calibration and the known peak energy of the transuranic nuclide of interest as well as the known peak energies of the radon progeny. In addition, we assume that the spectrum is a linear combination of single energy response functions. This means that at each "valley" channel, X_n, its contents are a linear combination of the counts from the tails of the peaks to the right of it, i.e. the counts at X_3 are caused by the 8.78 MeV peak, at X_2 by the 8.78 MeV and the 7.68 MeV peaks, etc. Furthermore, we assume that the tail of each peak below the "valley" point to the left of it can be described by a single exponential function of the form

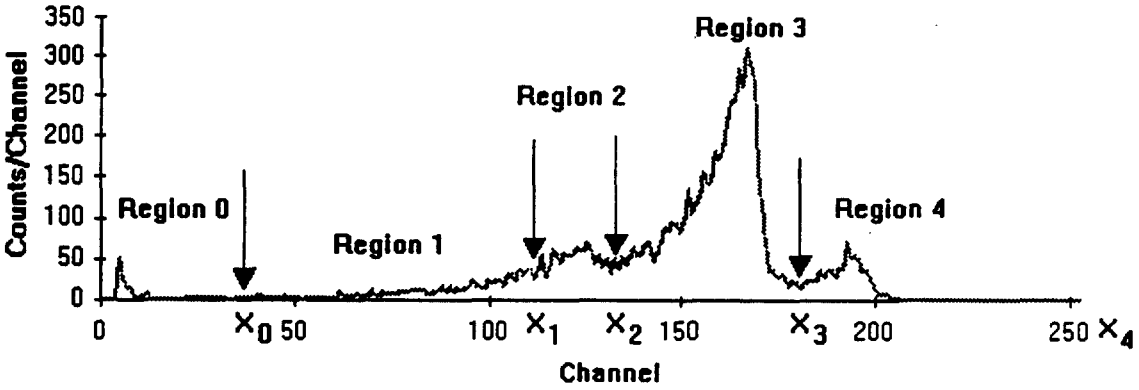

Figure 1 Typical CAM spectrum.

$$Y_i = e^{m \cdot X_i + b} \tag{1}$$

where Y_i are counts in channel X_i, and m and b are constants.

According to this model, the 8.78 MeV tail will pass through values that represent only its contribution at X_3 and X_0. For a more representative value, particularly since the low counts of the CAM spectra mean poor statistics, we define the contribution at channel X_3 as an average of 2k+1 channels about it, that is

$$Y_{3(av)} = \frac{1}{2k+1} \sum_{i=X_3-k}^{X_3-k} Y_i \tag{2}$$

where we choose k = 2.

At channel X_0, we define the contribution due to the 8.78 MeV peak, $Y_{0(8.78)}$, as

$$Y_{0(8.78)} = \frac{\sum_{i=X_3}^{X_4} Y_i}{\sum_{i=X_0}^{X_4} Y_i} \cdot Y_{0(av)} \tag{3}$$

where $Y_{0(av)}$ is calculated around X_0 using Equation (2). In principle, the numerator in Equation (3) should include the counts in the tail portion of the response function as well. However, due to the fact that the contribution of the tail to the total sum is rather small, we assume Equation (3) to be a good approximation.

The tail function of the 8.78 MeV peak can now be determined by substituting X_3, $Y_{3(av)}$, X_0, and $Y_{0(8.78)}$ into Equation (1) and solving for the coefficients $m_{8.78}$ and $b_{8.78}$. After subtracting the

response function of 8.78 MeV peak from the spectrum channel by channel, the process is then repeated for the 7.68 and 6.05 MeV peaks. The transuranic net area is the remainder after all three background peaks have been subtracted, namely:

$$A_{Pu} = \sum_{i=X_0}^{X_1-1} \left(Y_i - e^{m_{8.78}X_i + b_{8.78}} - e^{m_{7.68}X_i + b_{7.68}} - e^{m_{6.05}X_i + b_{6.05}} \right) \qquad (4)$$

Theoretically, the counts in the tails are Poisson distributed; however, the tail integral is not. To be conservative, we use the net area of all four peaks to estimate the net area uncertainty for the transuranic counts. We then require that its area must exceed the area uncertainty estimate multiplied by a desired confidence factor for the transuranic nuclide to be detectable.

All of the background compensation calculations are performed by a separate control unit at the end of a preset count cycle for each sampling head connected to it. Whether an alarm will be indicated is dependent on whether the detected transuranic count rate translates to an exposure (in DAC-hrs) that is higher than the currently selected "slow" alarm limit. In addition, each sampling head calculates a "fast" alarm every 30 seconds based on the counts collected within the last 30 seconds. The "fast" alarm is indicated if the number of counts in region 1 exceeds a preset level, and the ratio of average counts per channel in region 1 to the average counts per channel in the window from X_1 to the 6.0 MeV peak exceeds a factor of two.

III. Experimental Procedures

The tests to verify the performance of the new CAM sampler were primarily conducted at the Texas A&M wind tunnel facility. The experimental protocol on how to verify the penetration of aerosol particles as a function of the aerodynamic equivalent size has been previously described in detail.[6] It basically involves generating a uniform non-radioactive, but measurable (fluorescent tracer) aerosol concentration profile in the test section of the wind tunnel through the use of a vibrating jet atomizer.[8] The aerosol is then simultaneously sampled with the CAM sampling head and an isokinetic probe fitted with a filter collector. At the conclusion of the test filters from the CAM and the probe are removed and the aerosol penetration is determined from the ratio of the masses of the fluorescent tracer collected by the CAM and the isokinetic probe, and the flow rates through the two samplers. The size of the aerosol produced by the atomizer is verified with a microscope both at the beginning and at the end of each test. At least three replicate tests were run at each aerosol size to obtain a measure of the reproducibility of the experiment and to provide an uncertainty estimate for the result.

The tests to verify uniformity of deposition consisted of

operating the CAM sampler in the wind tunnel for a slightly longer time than necessary for the penetration studies (15 to 45 minutes) to collect a sufficient mass of the tracer such that it would be quantifiable even with small subsamples. The filter was then cut into 20 subsamples and quantified for uniformity of deposition. This experiment also included at least three replicate measurements at each test condition to obtain an estimate of the reproducibility of the experiment.

To establish how well the diffusion screen removes radon daughters, we pumped filtered, clean air through 200 liters of high-grade uranium ore to spike it with radon. The air was then pumped through a baffled chamber to mix it thoroughly and to allow the radon progeny to form. At the other end of the chamber, the air was pulled through a CAM unit and an open-faced filter. The CAM unit and the open-faced filter were operated for several 5 minute periods, first at 28.3 L/min and then at 56.6 L/min air flow. Within 1 minute of the termination of each exposure, both filters were counted to establish their activities using the three-count technique of Nazaroff[9]. The amount of removal of the unattached fraction can be calculated from the ratio of the ^{218}Po activities in the two filters. These results have been previously reported.[1]

In the present studies, we used the chamber with the radon progeny generator to test the ability of the background compensation algorithm to issue reliable "slow" alarms. For this purpose, we generated two different types of radon environments. To simulate clean laboratory environments, the air in the mixing chamber air was kept clean to keep the radon daughters in a mostly unattached form. To simulate less clean environments, we injected aerosols into the mixing chamber to act as condensation centers to make the radon progeny appear to the CAM in a mostly attached form. The unattached radon daughter environment was tested with and without the diffusion screen in place. A summary of the three different types of environments (A, B, and C) is shown in Table 1. The amount of radon daughters in the air stream was established from the activity measured from the open-faced filters. The values indicated in the table represent the radon concentration outside the CAM unit. Since we had previously established[1] that the diffusion screen removes 99% of the freshly formed (unattached) radon daughter products from the air stream, the percentage of attachment also shown in Table 1 can easily be calculated from the ratio of the activity in the open-faced filter and the activity in the filter inside a CAM unit with the diffusion screen in place.

The CAM unit was operated at a flow rate of 56.6 L/min for a 5 minute count cycle in these three environments with a clean filter as well as with a filter that had previously been loaded with a small amount of plutonium. Two different plutonium loaded filters, one with approximately 15 cpm and the other with about 35 cpm of plutonium were used for these tests. Neither one exceeds the 8 DAC-hr limit under such conditions. We therefore set the alarm threshold low enough, such that if plutonium was detected, the unit would issue an alarm. At each count cycle, the resulting spectrum

Table 1. Radon environments used to test the slow release alarm.

Environment Type	Radon Progeny in Ambient Air (pCi/L) RaA	RaB	RaC	Percent of Radon Progeny Attached RaA	RaB	RaC
A (Unattached RD, Screened Inlet)	1.025 ±0.095	0.065 ±0.039	-0.032 ±0.029	2.4 ±2.3	0.6 ±14.9	-46.2 ±48.4
B (Unattached RD, Unscreened Inlet)	0.591 ±0.074	0.023 ±0.030	-0.002 ±0.022	3.1 ±2.9	3.7 ±6.0	-191.1 ±2370
C (Attached RD, Unscreened Inlet)	1.706 ±0.139	0.331 ±0.060	0.101 ±0.048	90.6 ±10.9	107.9 ±28.3	137.3 ±81.2

was analyzed for both the "slow" and the "fast" alarm. For this particular test, the sampling head did not have the capability to calculate the "fast" alarm, so the fast alarm was calculated at the end of the count cycle for comparison only. In actual usage of the CAM system, the "fast" alarm will be calculated in the sampling head and can result in a truncation of the count cycle. In a separate test at Los Alamos, we created an environment with a pre-loaded filter where the exposure exceeded 8 DAC-hrs.

IV. Results and Discussion

The results of the aerosol penetration study for the Canberra prototype are shown in Table 2. For comparison, the results for the original Los Alamos/Texas A&M model are shown for one of the cases. The results for the 56.6 L/min flow rate case are also shown graphically in Figure 2. In the figure, the curves represent polynomial fits through the data points. It is clear that the Canberra prototype exhibits the same characteristics as the original design.

Table 2. Aerosol penetration characteristics of the original prototype and the Canberra prototype.

Wind Speed (m/s)	Air Flow (L/min)	CAM Prototype	Aerodynamic Particle Size (μm)	Penetration Percent	Standard Deviation Percent
1.0	56.6	Los Alamos	5	101.9	3.2
			10	79.8	0.6
			15	54.4	1.4
1.0	56.6	Canberra	5	98.6	1.7
			10	81.2	2.0
			15	63.3	1.3
0.5	56.6	Canberra	3	95.1	2.5
			5	94.2	0.9
			10	86.6	1.6
			15	61.3	0.8
			20	38.8	0.8
0.5	28.3	Canberra	3	95.0	3.7
			5	88.9	1.9
			10	75.3	1.3
			15	42.1	0.4
			20	18.3	0.6

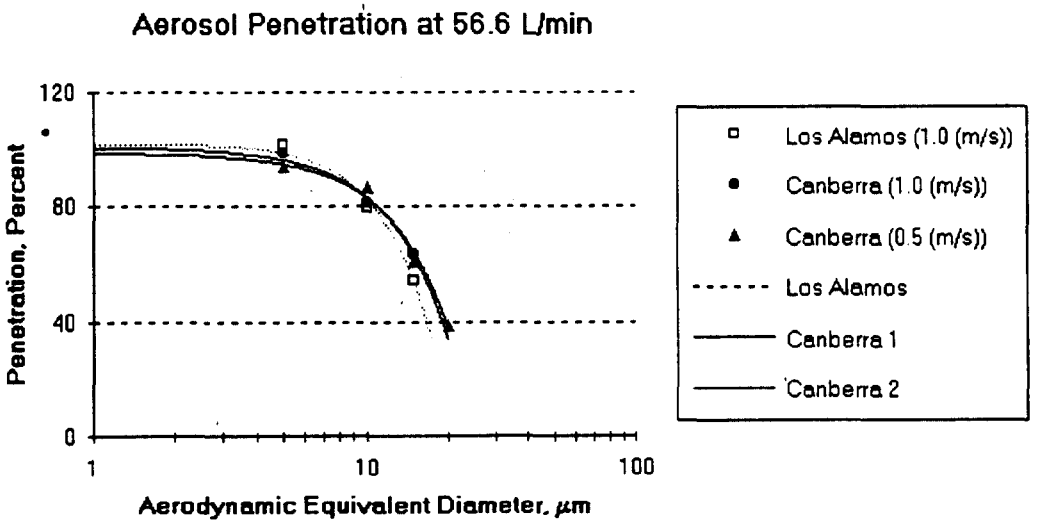

Figure 2 Comparison of the aerosol penetration results from the Los Alamos/Texas A&M prototype and the Canberra prototype.

The results of the uniformity of deposition studies for the Canberra prototype are summarized in Table 3. Here, the coefficient of variation represents the standard deviation of the aerosol mass per unit area in the subsamples to the mean mass/area on the complete filters. The values are normalized to a mean of unity and established with a wind speed of 0.5 m/s for 10μm particle size. For comparison, we have also included the results for the Los Alamos/Texas A&M prototype. While the measurements were not under identical conditions, it can clearly be seen that the results for the Canberra prototype are at least as good as those of the original design.

Table 3. Uniformity of aerosol deposits.

CAM Prototype	Wind Speed (m/s)	Inlet Configuration	Flow rate (L/min)	Coefficient of variation (%)
Canberra	0.5	Radial	56.6	7.9
		In-line	56.6	8.8
			28.3	5.4
Los Alamos	0.3	Radial	56.6	14.6
			28.3	14.1
		In-line	56.6	13.7

The results of the background compensation tests are shown in Table 4. As can be seen from the table, no false alarms were observed for the clean filters in any of the environments for the "slow" alarm algorithms. For the pre-loaded plutonium filters, it indicates the presence of the transuranic counts quite reliably in all environments. Comparing the results for environments A and B, it is also evident that the presence of the diffusion screen enhances the capability of the algorithm.

The "fast" alarm calculations are based on a simplified algorithm and are normally done in the sampling head. For this particular test, the sampling head was not equipped with the "fast" alarm capability and the results shown in Table 4 are shown for full count cycles for illustration only. However, it is noteworthy that there are no false alarms for the clean filters. Furthermore, the presence of the diffusion screen helps the "fast" alarm algorithm as well, as evidenced by the results from environment A.

Table 4. Fast and slow alarm results.

No. of Measurements	Environment Type*	Filter Type	Alarm (True/False) Fast	Slow
177	A	Clean	0/177	0/177
94	A	Pre-loaded	7/84	93/1
87	B	Clean	0/87	0/87
76	B	Pre-loaded	0/76	71/5
46	C	Clean	0/46	0/46
12	C	Pre-loaded	0/12	12/0

* See Table 1.

The results for the separate exposure test at Los Alamos are shown in Figure 3. The first 15 measurements were done with no air flow to establish the count rate for the pre-loaded plutonium. For the rest of the measurements, the count cycle time was set to 15 minutes and the air flow to about 47.5 L/min. It can be noted that the output from the CAM is a set of very consistent readings for both the counts/min and the DAC-HRS.

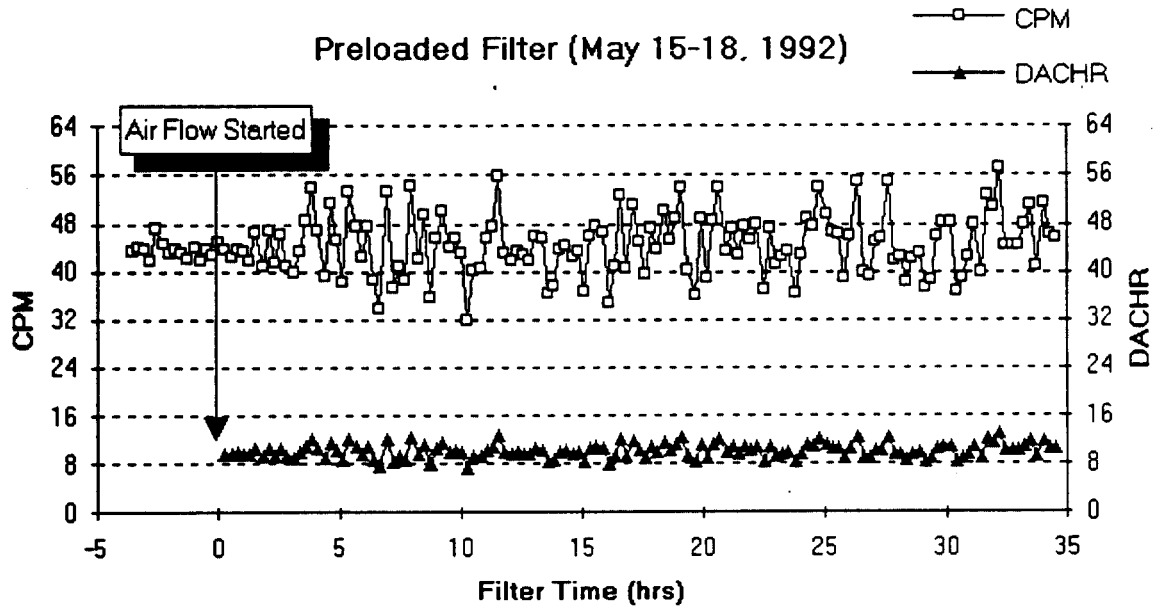

Figure 3 Observed net plutonium count rate and the calculated DAC-hr exposure for a pre-loaded plutonium filter.

V. Conclusion

As can be seen from the results presented in this study, the Canberra CAM unit clearly meets the design criteria of the original Los Alamos/Texas A&M CAM design. Furthermore, in tests conducted in a variety of environments, the new background compensation algorithm has proven to give reliable and accurate results at or near the 8 DAC-hr exposure limit.

VI. References

1. McFarland, A.R., Rodgers, J.C., Ortiz, C.A. and Moore, M.E., "A continuous sampler with background suppression for monitoring alpha-emitting aerosol particles", Health Physics, Vol. 62, pp. 400-406, (1992).

2. "Radiation Protection of Occupational Workers", U.S. Department of Energy, DOE Order 5480.11 (1988).

3. McFarland, A.R., Ortiz, C.A. and Rodgers, J.C., "Performance evaluation of continuous air monitor (CAM) sampling heads", Health Physics, Vol. 58, pp. 275-281, (1990).

4. Biermann, A. and Valen, L., "CAM particle deposition evaluation", in Griffith, R.V. ed. Hazards Control Department Annual Technology Review, Livermore, CA. Report UCRL-5007-83, 1983.

5. Rodgers, J.C. and McFarland, A.R., "Factor affecting the performance of alpha continuous air monitors". Presented at the 34th Health Physics Society Annual Meeting, June 1989. Report LA-UR-89-7920, 1989.

6. McFarland, A.R.; Bethel, E.L.; Ortiz, C.A.; Stanke, J.G. "A CAM sampler for collection and assessment of alpha-emitting aerosol particles", Health Physics, Vol 61, pp. 97-103, (1991).

7. M. J. Koskelo, "Interactive Alpha Spectroscopy on Personal Computers", Nucl. Instr. & Meth., Vol. A286, pp. 433-438, (1990).

8. Berglund, R.N. and Liu, B.Y.H, "Generation of monodisperse aerosol standards", Environ. Sci. & Technol. Vol. 7, pp. 147-153, (1973).

9. Nazaroff, W.W., "Optimizing the total-alpha three-count technique for measuring concentrations of radon progeny in residences", Health Physics, Vol. 46, pp. 275-281, (1984).

DISCUSSION

FRENQUELLI: In a test of attached and unattached radon conditions, I did not see data on attached radon with the screen inlet. What predictions would you be making for that case?

KOSKELO: As far as we have been able to determine, I did not include that because our tests indicate that if the screen is in place and the radon daughters are mostly in an attached form, it doesn't do anything at all. It is the same thing as if the diffusion screen was not in place. Often, in very dusty environments, where you might see that sort of thing, the inert dust would load up the diffusion screen and you are better off just taking it off.

SCHOLTEN: I would like to ask the level of sensitivity of these methods. You gave an alarm setting of 8 DAC•hrs. If you sample for a week, what will be the sensitivity of detection?

KOSKELO: The sensitivity of the detection depends entirely on the radon level, which can vary considerably. What I did not mention specifically, is that you can set what we call a collection cycle time. That is, the unit will measure for a desired period of time, let's say one hour, and then look at the spectrum and analyze it and then erase it. So, any prior radon concentration that you may have had in your spectrum will get removed. We have looked at different situations but we have not actually done measurements with extremely high radon daughter concentrations. However, we feel that the current sensitivity, according to our calculations, at 10 pCi/L of radon inside the unit, depending upon the collection cycle that you pick, will be roughly 5-10 DAC•hours. Ten pCi/L according to my understanding is an extremely high concentration of radon daughters. I would like to also point out that if it is all in unattached form, 10 pCi/L inside the unit means about 100 pCi/L outside the unit since 90% or more will be removed by the screen.

AEROSOL PARTICLE LOSSES IN SAMPLING SYSTEMS*

B.J. Fan, F.S. Wong, C.A. Ortiz, N.K. Anand and A.R. McFarland

Aerosol Technology Laboratory, Department of Mechanical Engineering,
Texas A&M University, College Station, TX 77843.

Abstract

When aerosols are sampled from stacks and ducts, it is usually necessary to transport them from the point of sampling to a location of collection or analysis. Losses of aerosol particles can occur in the inlet region of the probe, in straight horizontal and vertical tubes and in elbows. For probes in laminar flow, the Saffman lift force can cause substantial losses of particles in a short inlet region. An empirical model has been developed to predict probe inlet losses, which are often on the order of 40% for 10 μm AED particles. A user-friendly PC computer code, DEPOSITION, has been setup to model losses in transport systems. Experiments have been conducted to compare the actual aerosol particle losses in transport systems with those predicted by the DEPOSITION code.

I. Introduction

Aerosol particle sampling from stacks and ducts in the nuclear industry is usually conducted in a somewhat different manner than in other applications. Typically, in the nuclear industry, a sample is extracted from a stack or duct and transported to either a continuous air monitor (CAM) or a filter air sampler (FAS). If the amount of radioactivity detected by the CAM exceeds a preset level, the CAM will signal an alarm which will serve as the basis for initiating precautionary or emergency procedures. Aerosol samples collected with the FAS units are analyzed in a laboratory subsequent to the collection process and are intended to provide integrated results on the emissions of radionuclides during the sampling period. It is highly important that aerosol losses in the sample transport lines be minimal in order that CAMs can provide prompt and reliable alarms and that FASs yield data which accurately characterize the emissions. In contrast, losses in the aerosol transport lines in industrial stack sampling applications may not be of significance. For example, the U.S. Environmental Protection Agency standard method for stack sampling[1] involves periodic sampling on a batch basis. At the completion of a sampling experiment, the probe and transport tubing are washed to recover the losses, which are then taken into account as are the aerosol particles which penetrate the transport system. Because of the nature of the particles and the methodology of the sampling process, routine recovery of wall losses in aerosol transport systems is not a viable alternative in nuclear sampling applications.

In general, an aerosol transport system consists of an inlet, straight sections of tubing which

*Funding was provided by the U.S. Nuclear Regulatory Commission under Contract Grants NRC-04-89-115 and NRC-04-89-353. Dr. Stephen A. McGuire is the monitor for both grants.

may be at various orientations to the horizontal plane, and elbows. Particle losses in inlets occur as a result of the Saffman lift force[2] and free stream turbulence[3]. For supramicrometer-sized aerosol particles, losses in vertical tubes take place because of turbulent deposition and for submicrometer aerosol particles the losses are generally due to Brownian diffusion. For tubes which are non-vertical, the gravitational sedimentation can cause losses of supramicrometer particles. The losses in elbows are primarily due to inertial effects.

A. Inlets

The losses of aerosol particles in inlets can be substantial. It is often assumed that the use of an isokinetic inlet will assure the collection of a representative sample; however, several investigators have noted there are aerosol losses on the internal surfaces of isokinetic probes[4-7]. As an example of the magnitude of the losses, McFarland et al.[7] isokinetically sampled a 10 μm aerodynamic equivalent diameter (AED) aerosol at a flow rate of 170 L/min from a wind tunnel in which the mean velocity was 14 m/s. Thirty nine percent of the aerosol was lost to the probe walls. Isokinetic probes are included in the current version of the aerosol sampling standard used in the nuclear industry, ANSI N13.1[8]. We tested, in an aerosol wind tunnel, the sampling characteristics of an ANSI-type probe which had been fabricated by a DOE contractor. This probe, which differs from the standard ANSI design only through the inclusion of an enlargement of the flow stream immediately after the inlet section, Figure 1 a), is comprised of both a true inlet and an elbow. The wall losses for this probe are shown in Figure 1 b), where it may be noted that over a range of velocities of 6 - 20 m/s, the losses of 10 μm AED particles varied from 60 - 80%. For this ANSI-type probe, the wall losses could have been reduced by expanding the flow cross section considerably more upstream of the elbow.

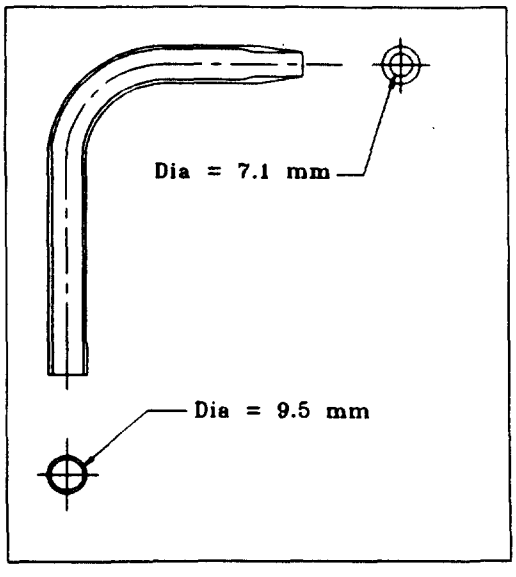

Figure 1 a). An ANSI-type probe which was designed for use in a nuclear sampling application.

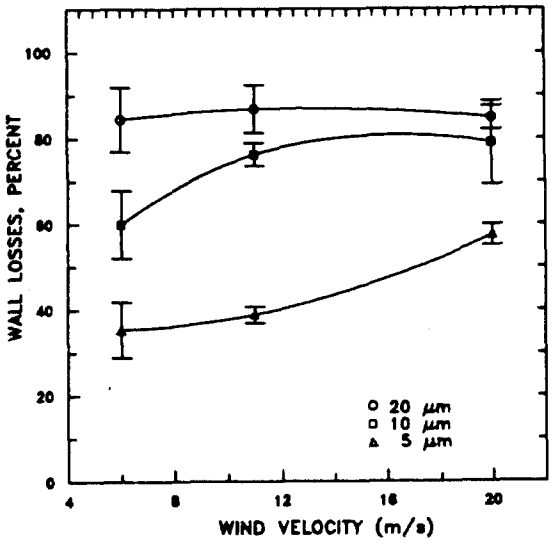

Figure 1 b). Wall losses in the ANSI-type probe determined from wind tunnel experimentation.

Various explanations have been forwarded for the high wall losses which can take place in the inlet region of a probe. Okazaki and Willeke[5] developed a model to explain the losses in laminar flow situations, where they proposed that particles strike the tube walls as a result of sedimentation in the developing fluid flow boundary layer. However, losses are also noted in vertically-oriented probes[6], while their model would predict zero losses for vertical probes. Fan et al.[9] considered the effect of the Saffman force in the entrance region of a probe and showed that losses can occur within a short region of the probe inlet as a result of this mechanism. The Saffman force acts to drive particles towards a wall when there is flow shear and the particles are decelerating in the shear layer. For non-turbulent flow, the Saffman force will generally be the dominant mechanism in causing wall losses; however, if the free stream flow is turbulent, the turbulent eddies which are drawn into the inlet can drive particles to the wall. This mechanism of particle deposition was experimentally investigated by Wiener and Willeke[3].

Fan et al.[10] conducted a series of wind tunnel experiments in order to develop a data base for construction of a semi-empirical model for wall losses in inlets. They correlated wall losses with the Stokes number, particle Froude number and a particle lift number (Pl), where the latter parameter reflects the influence of the Saffman force. Their correlation is:

$$WL = \frac{177\ Rs^{0.559}}{\left(1+\frac{L}{Fr}\right)^{9.19}\ Re^{0.216}} \tag{1}$$

where: WL = percentage of aerosol lost to the walls, L = dimensionless probe length (actual length/probe diameter), Fr = particle Froude number, Re = flow Reynolds number, and Rs = a dimensionless parameter given by:

$$Rs = \frac{2\ Stk}{\sqrt{Pl}} \tag{2}$$

where: Stk = particle Stokes number, which is represented by:.

$$Stk = \frac{C\rho_p D_p^2 U_m}{9\mu d_t} \tag{3}$$

where: C = Cunningham slip correction, ρ_p = particle density, D_p = particle diameter, U_m = mean gas velocity in inlet, μ = gas dynamic viscosity, and d_t = internal diameter of the inlet at the entrance section. The particle lift number is given by:

$$Pl = \frac{2\tau_d U_m}{d_t} \tag{4}$$

where: τ_d = particle deflection time, which is a measure of the time for the particle to adapt to the Saffman lift force. In turn, the particle deflection time is given by:

$$\tau_d = \frac{0.115 \rho_p D_p \sqrt{d_t}}{\sqrt{\rho \mu U_m}} \tag{5}$$

where: ρ = air density. The particle Froude number is defined as:

$$Fr = \frac{2U_m^2}{g d_t} \tag{6}$$

where: g = local acceleration due to gravity. Also, the flow Reynolds number is:

$$Re = \frac{\rho U_m d_t}{\mu} \tag{7}$$

The model of Fan et al.[10] is based on probes with straight internal cross sections and the data base was comprised of only particles with sizes of 10 and 20 μm, so it cannot be used as a general predictive tool for all probe applications; nevertheless, it does provide the basis for estimating internal wall losses in probes.

In addition to problems created by internal wall losses, aerosol samples can also be non-representative if the sampling is performed under anisokinetic conditions. Anisokineticity results if either the probe is not aligned isoaxially with the air stream or if the velocity at the probe inlet is not matched to that of the flow stream. The semi-empirical model of Vincent et al.[11] can be used to predict sample bias caused by anisokinetic effects.

B. Straight Tubes

The flow rate and tube sizes employed in aerosol transport systems are such that the flow Reynolds numbers are usually in the transitional or turbulent regime; hence, aerosol deposition can be analyzed from the standpoint that the flow is continually stirred. This permits the penetration of aerosol through a tube to be expressed as:

$$P = e^{\frac{-\pi d_t V_e L_t}{Q}} \tag{8}$$

where: P = ratio of aerosol concentration at the tube exit plane to that at the tube inlet plane, V_e = effective particle deposition velocity, and Q = air flow rate through the tube. The effective particle velocity is the vector sum of the deposition velocity due to gravity and that due to the combination of turbulent and Brownian diffusion. Anand et al.[12] have presented an analytical solution for the method of combining the deposition velocity components.

The turbulent deposition velocity was first modeled by Friedlander and Johnstone[13] who developed what has come to be known as a "free-flight" model. They assumed that turbulent eddies transport particles to the vicinity of the wall, and if the particles are brought to within one stopping distance of the wall, free-flight will cause deposition to take place. The characteristic velocity they used in the stopping distance was the root-mean-square eddy velocity of the flow

outside of the boundary layer. Also, they assumed an equality of eddy diffusivity and particle diffusivity. The conducted experiments to determine the particle deposition velocity and their model and experiments agreed quite well. Davies[14] re-derived the free-flight turbulent deposition model with assumptions that were more plausible than those of Friedlander and Johnstone, including a more realistic value for the particle velocity at the start of the free-flight process; however, his model does not agree well with experimental data[15]. Beal[16] made modifications to the Friedlander and Johnstone model which included an assumption that the aerosol concentration was non-zero in the region between the start of free-flight and the wall. In addition, Beal's model takes into account Brownian diffusion, which the model of Friedlander and Johnstone did not. Onda[15] reviewed existing models and reported that the model of Beal best fit the experimental data.

C. Elbows

The analysis of particle deposition in elbows is complicated by the fact that there is a secondary flow setup as the fluid passes through the elbow. This secondary flow appears as a set of counter-rotating vortices in which the secondary flow goes from the inside of the bend to the outside along the tube diameter, and goes in the reverse direction at the tube circumference. For a two dimensional bend, with the radius of curvature much greater than the channel width, and with the aerosol assumed to be stirred as it flows around the bend, the particle deposition depends only on the Stokes number based on mean flow velocity and tube diameter.

Pui et al.[17] experimentally determined wall losses in circular elbows over a range of Stokes number and Reynolds number and obtained the empirical correlation of:

$$P = 10^{-0.963\,Stk} \tag{9}$$

The correlation is for a turbulent flow with a curvature ratio, R_o, greater than 5, where:

$$R_o = \frac{2R}{d_t} \tag{10}$$

Here, the parameter R is the radius of curvature of the tube bend.

For the laminar flow regime, Cheng and Wang[18] developed an analytical model which considered the particle trajectories but did not take into account secondary flow. Pui et al. noted the model of Cheng and Wang matched their data at a Reynolds number of 1000, but not at a Reynolds number of 100. Tsai and Pui[19] numerically analyzed particle trajectories in laminar flow through a tube bend and developed a correlation of aerosol penetration with the Stokes number, curvature ratio and the Dean number, De, where the latter is defined as:

$$De = \frac{Re}{\sqrt{R_o}} \tag{11}$$

Their model quite well fit the data for the laminar regime which were gathered previously by Pui et al[17].

II. Deposition Software

A. Basis of the Code.

We developed a user-friendly PC-based software program to model particle deposition in transport lines[20]. This code, DEPOSITION 2.00, calculates aerosol particle losses in systems comprised of inlets, straight tubes and elbows under the assumption that the loss in each component is independent of the presence of any other component. Under this assumption, the overall penetration, P_T, through a transport system comprised of N components is:

$$P_T = \prod_{i=1}^{N} P_i \tag{12}$$

where P_i is the penetration through the ith component. If the aerosol is polydispersed, the overall penetration is calculated from:

$$P_T = \sum_j \prod_i \frac{m_j}{M} P_{ij} \tag{13}$$

where P_{ij} is the penetration of the jth particle size through the ith component and m_j/M is the mass fraction of aerosol in the jth particle size interval. The submodels used to calculate penetration through inlets are those of Vincent et al.[11] for anisokinetic effects and Fan et al.[10] for internal losses in isokinetic probes. The model of Beal[16] is employed to calculated the deposition velocity due to the effects of Brownian and turbulent diffusion in straight tubes. Use is made of the model of Anand et al.[12] to determine losses due to the combined effects of sedimentation and diffusion. For elbows, the model of Tsai and Pui[19] is used if the Reynolds number is < 1100, otherwise the model of Pui et al.[17] is utilized.

The code offers several options which permit calculations for retrospective analysis of existing sampling lines and for design of new systems. In particular, the options are:

1. Calculate Actual Penetration for an Existing Transport System. Under this option, the user inputs the tube geometrical and operational parameters (free stream velocity, sample flow rate, particle size distribution, inlet size, tube size, orientation and length of each straight section and the number of elbows). The program then computes the penetration of aerosol through each component and the overall penetration.

2. Calculate Optimum Diameter. Here, the user gives the same information as in the first option, with the exception of the tube diameter. The computer will then step through different tube sizes until it locates a size that provides a maximum penetration. For a maximum to exist, there must be at least one non-vertical straight tubing component in the system.

3. Maximum Penetration. Consider a transport system which connects two points in space and which samples a given particle size distribution at a particular flow rate. Under this option, the computer will calculate the maximum penetration which could be achieved by any system for this application. The results can be used as a benchmark against which to compare any other transport system.

4. Calculate Penetration with Varying Parameters. This option operates on the same basis as Option 1, except that the tube diameter, flow rate, or particle size can be varied over a range of values. Output is written to an ASCII file, which can be imported into a PC spreadsheet or graphing application.

B. Example of an Application.

To illustrate the use of the DEPOSITION 2.00 code, assume the sampling system shown in Figure 2 is designed to isokinetically sample a flow rate of 56.6 L/min (2 cfm) from a free stream which has a velocity of 20 m/s (65.6 ft/s). Suppose the tube is 15.75 mm inside diameter (3/4-inch outside diameter x 0.065-inch wall), what is the penetration of 10 μm AED aerosol particles through the system?

The inputs to the DEPOSITION 2.00 code and the corresponding outputs are shown in Table 1. The overall penetration for this example, 27.3%, is low for a system of its geometrical layout due to the choice of tube size. Were we to use Option 2 to provide an optimal tube size, the results would be a tube diameter of 34 mm and a corresponding penetration of 72.6%.

Table 1. Input parameters and output values for the example transport system shown in Figure 2. Option 1 of DEPOSITION: Existing Transport System.

INPUT PARAMETERS	OUTPUT VALUES
Flow rate: 56.6 L/min	Penetration through inlet: 81.8%
Tube diameter: 15.75 mm	Penetration thru element 2: 98.5%
Number of components (inlet is element number 1): 6	Penetration thru element 3: 66.0%
Particle density: 1 g/cm^3	Penetration thru element 4: 85.7%
Is inlet isokinetic? Yes	Penetration thru element 5: 66.0%
Free stream velocity: 20 m/s	Penetration thru element 6: 90.7%
Angle between free stream and inlet: 0°	OVERALL PENETRATION: 27.3%
Element 2: Tube, 0.2 m long, 0° from horizontal	
Element 3: Elbow, 90° angle	
Element 4: Tube, 2 m long, 0° from horizontal	
Element 5: Elbow, 90° angle	
Element 6: Tube, 2 m long, 90° from horizontal	

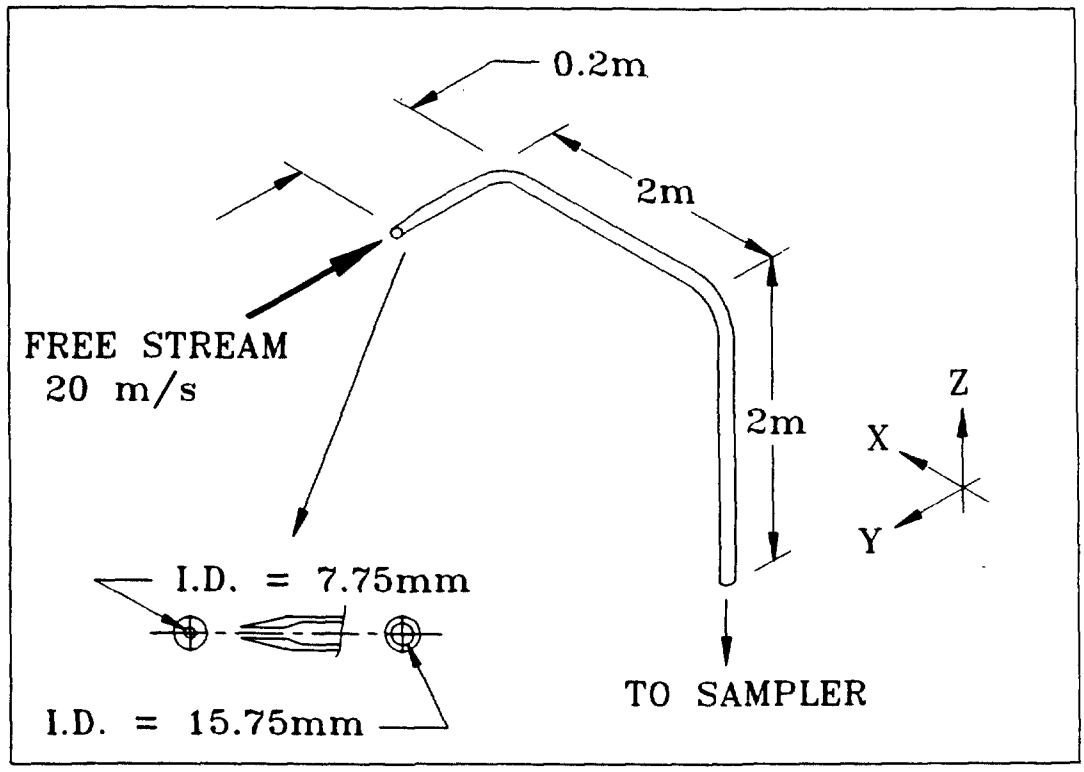

Figure 2. Layout of example aerosol transport system

III. Comparison of Numerically Predicted Penetration with Experiment Results

McFarland et al.[21] conducted wind tunnel tests with the model transport system shown in Figure 3. a) and made comparisons of the experimentally observed penetration with that predicted by the DEPOSITION code. They conducted all tests at a free steam velocity of 3 m/s. Flow rates through the system were 70 and 130 L/min and the inlet was operated parallel and perpendicular to the free stream. Typical results are those shown in Figure 3. b), which show the penetration as a function of aerodynamic particle diameter for a flow rate of 130 L/min with the inlet oriented parallel to the free stream.

Wong[22] constructed model aerosol transport loops with the same geometrical layout as that designed and tested earlier by Strom[23]. He tested the systems with aerosols and compared the results with those predicted by the DEPOSITION code and, where possible, with the experimental results measured by Strom.

Strom, in a pioneering effort with an aerosol transport system, setup a sampling loop in the vertical plane which consisted of four 16.8 mm diameter tubes each 2 m long which were connected by three elbows. Monodisperse aerosols were drawn into the tube and the penetration was determined for different flow rates. Strom plotted the penetration as a function of flow

Reynolds number and noted that for a constant particle size, there was a maximum of the penetration curve, and that these maxima all occurred at a Reynolds number of 2800. This value of the Reynolds number has been termed the "flow of best transmission," and has been used by some designers as a criterion for sizing aerosol transport lines. The DEPOSITION code does not predict such a "flow of best transmission," so Wong investigated the concept by first repeating the tests of Strom using a tube of approximately the same size as that used by Strom, and then conducted additional experiments with a tube of a different size.

The data of Wong for a Strom-type loop with a tube diameter of 15.9 mm are shown in Figure 4. a). From this curve it may be noted that the penetration maxima for particle sizes of 8, 10 and 15 μm AED all occur at a Reynolds number of approximately 2800. The Reynolds number in Wong's experiments was varied by changing the flow rate through the tube. In contrast to the results he obtained with a 15.9 mm inside diameter tube, when Wong tested a Strom-type loop with a 26.9 mm tube, the maximum penetration values were associated with Reynolds numbers of 5600, 3800 and 3300 for particle sizes of 8, 10 and 15 μm, respectively (Figure 4 b). This suggests that Strom's "flow of best transmission" is only appropriate for a single tube size.

A comparison of the data of Wong with the predictions from the DEPOSITION code for 10 μm AED aerosol particles are shown in Figures 5 a) and b) the 15.9 and the 26.7 mm inside diameter tubes. Again, in these figures, the penetration is plotted against the Reynolds number, where the Reynolds number was varied by changing the flow rate.

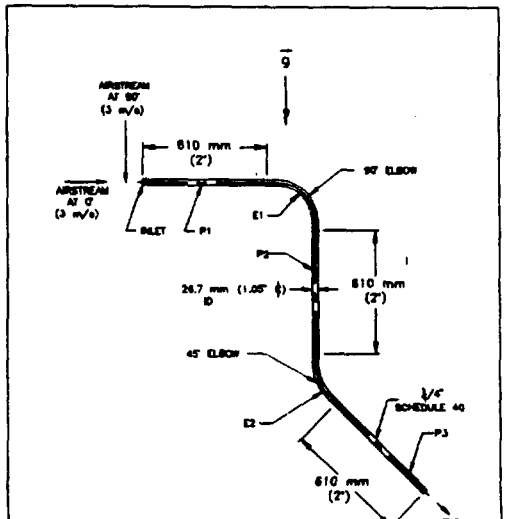

Figure 3 a). Aerosol transport system tested by McFarland et al.[21] in a wind tunnel. Reprinted with permission from *Environ. Sci. & Technol.*, **1991**, *25*:1573-1577.

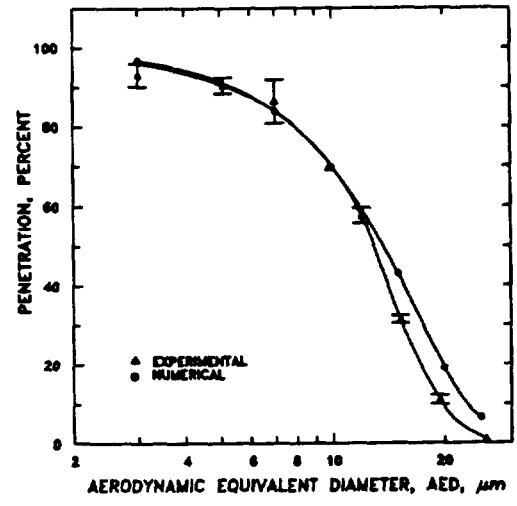

Figure 3 b). Results of wind tunnel testing of transport system. Flow rate = 130 L/min; inlet oriented parallel to free stream. Reprinted with permission from *Environ. Sci. & Technol.*, **1991**, *25*:1573-1577.

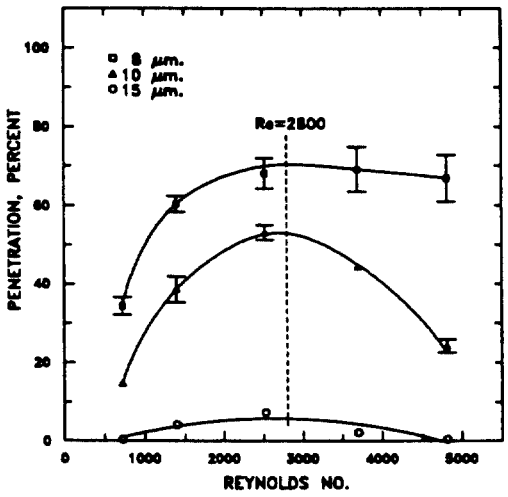

Figure 4 a). Data of Wong[22] for a Strom-type loop. Tube size = 15.9 mm inside diameter. Reynolds number was varied by changing the flow rate.

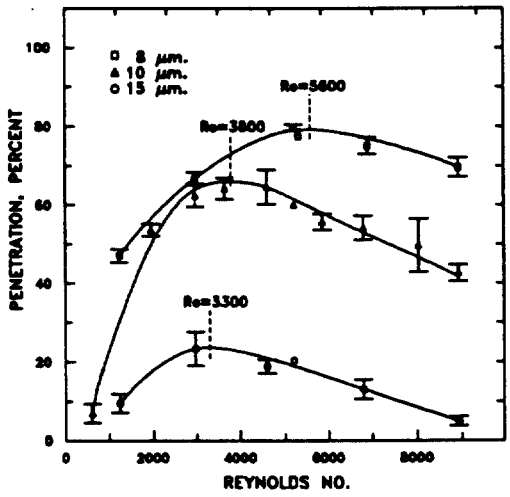

Figure 4 b). Data of Wong for a Strom-type loop with a 26.7 mm diameter tube. Note that the maximum penetration is not associated with a fixed value of the Reynolds number.

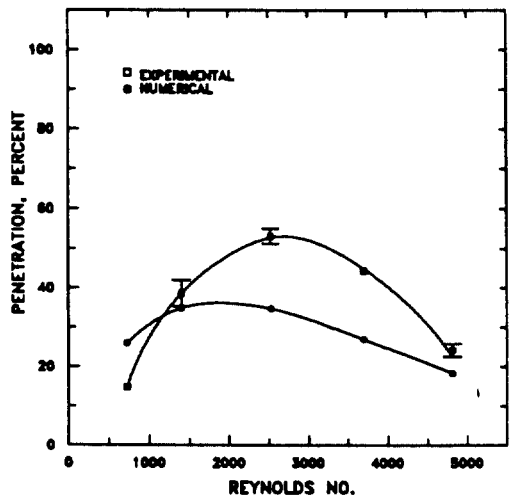

Figure 5 a). Comparison of the experimental data of Wong[22] with predictions from the DEPOSITION code. The system is a Strom-type loop with a tube diameter of 15.9 mm. Particle size = 10 μm AED.

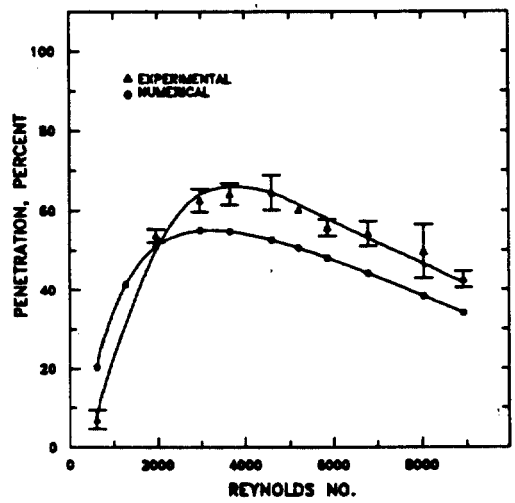

Figure 5 b). Comparison of Wong data and DEPOSITION code for a 26.7 mm diameter Strom-type loop. Particle size = 10 μm AED.

Wong[22] also conducted tests with 10 μm AED aerosol particles to characterize the penetration of aerosol through 2.4 m long horizontal tubes of different diameters (6.7 to 52.3 mm). He maintained the flow rate constant and determined the penetration. A comparison of his results with predictions from the DEPOSITION code is given in Figure 6. Both experiment and code show that there is an optimal tube diameter and both show that the penetration drops steeply if the tube is smaller than the optimal size and drops slowly if the tube diameter is larger than optimal. The steep decrease for smaller sized tubes is due to enhanced turbulent deposition and the decreasing penetration for larger sized tubes is due to the gravitational sedimentation.

IV. Summary and Discussion

In the nuclear industry, sampling lines can be quite long and there is a potential for significant losses of aerosol particles between the stack or duct where a sample is acquired and the location where samples are collected. For example, Glissmeyer and Sehmel[24] show data for nuclear reactor sampling lines in which the overall line length can be as long as 75 m with horizontal runs as long as 50 m.

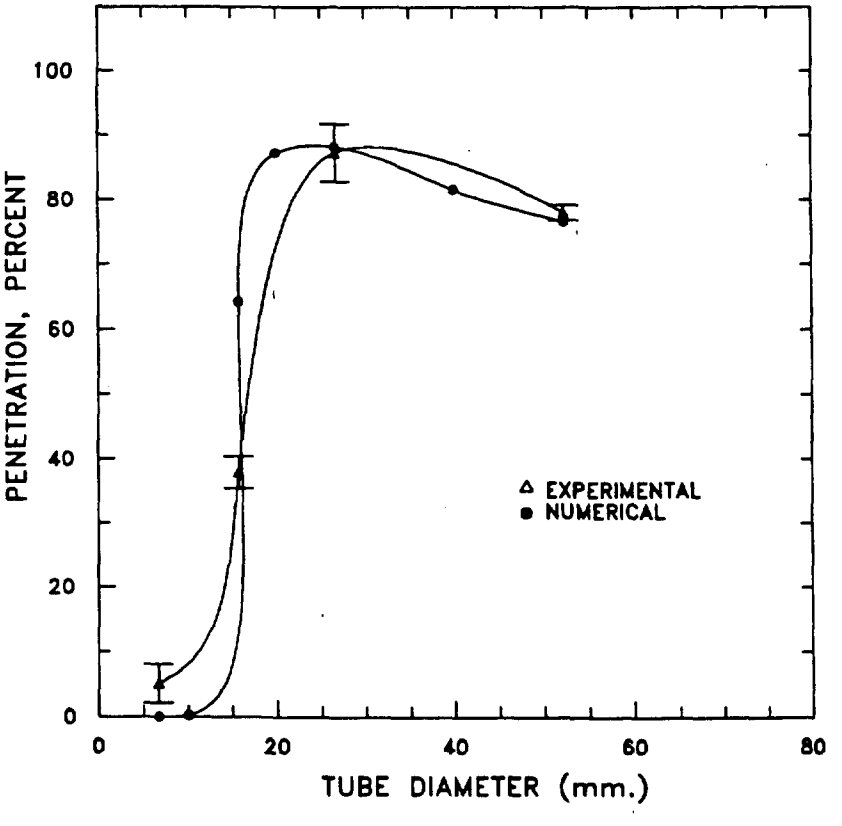

Figure 6. Penetration of 10 μm AED aerosol particles through 2.4 m long horizontal tubes of different diameters. Experimental data of Wong[22] are compared with predictions from the DEPOSITION code.

The DEPOSITION code allows estimates to be made of the aerosol losses through transport systems which consist of inlets, elbows and straight sections of tubing. The inlet losses include those which occur as a result of anisokinetic effects and internal wall losses. The losses in straight sections of tubing include the effects of gravitational settling and turbulent and Brownian diffusion. Losses in elbows are calculated from models for laminar and turbulent flow.

Experiments have been conducted to provide a data base for comparison with the DEPOSITION code. In the wind tunnel experiments of McFarland et al.[21], the test results and code predictions agreed well; although, for particle sizes > 10 μm AED the code predicted higher penetration values than those observed experimentally. Wong[22] setup two Strom-type aerosol transport loops[23] and conducted tests to both compare the results with those of Strom and with the predictions of the DEPOSITION code. Strom had observed a "flow of best transmission," when he tested a single tube diameter over a range of particle sizes and Reynolds numbers. His "flow of best transmission," corresponded to a Reynolds number of 2800. He varied the Reynolds number only through changing the flow rate. Wong duplicated the results of Strom when he used approximately the same tube size as Strom; however, when Wong used a different tube size, he did not obtain a "flow of best transmission." Instead, the maximum penetration varied with particle size. A comparison of the predictions of the DEPOSITION code with the experimental results of Wong for tests with 10 μm AED aerosol particles in Strom-type loops with tube sizes of 15.9 and 26.7 mm, showed the code correctly predicted the trends; but, the code overestimates the penetration at low flow rates (low Reynolds numbers) and underestimates at high flow rates. The DEPOSITION code shows good agreement with the results of Wong[22] from tests with horizontal tubes in which an optimal tube diameter was demonstrated for fixed values of particle size and flow rate.

V. References

1. U.S. Environmental Protection Agency. (1991). Code of Federal Regulations, 40 CFR 60. Appendix A - Test methods, Method 5; Determination of particulate emissions from stationary sources. U.S. Government Printing Office Washington, D.C.
2. Fan, B.J.; McFarland, A.R.; Anand, N.K. (1992). Aerosol particle losses in isokinetic sampling probe inlets. *Environ. Sci. & Technol. 26*:390-394.
3. Wiener, R.W.; Okazaki, K., Willeke, K. (1988). Influence of turbulence on aerosol sampling efficiency. *Atmospheric Environ. 22*:917-928.
4. Durham, M.D.; Lundgren, D.A. (1980). Evaluation of aerosol aspiration efficiency as a function of Stokes number, velocity ratio and nozzle angle. *J. of Aerosol Sci. 11*: 179-188.
5. Okazaki, K.; Willeke, K. (1987). Transmission and deposition behavior of aerosols in sampling inlets. *Aerosol Sci. and Technol. 7*:275-283.
6. Jayasekera, P.N.; Davies. C.N. (1980). Aspiration below wind velocity of aerosols with sharp edged nozzles facing the wind. *J. Aerosol Sci.* 535-547.
7. McFarland, A.R.; Ortiz, C.A.; Moore, M.E.; DeOtte, R.E., Jr.; Somasundaram, S. (1989). A shrouded aerosol sampling probe. *Environ. Sci. & Technol. 23*:1487-1492.
8. American National Standards Institute. (1969). Guide to sampling airborne radioactive materials in nuclear facilities. ANSI Standard N13.1-1969. American National Standards Institute, New York.

9. Fan, B.J.; McFarland, A.R.; Anand, N.K. (1992). Characterization of the aerosol particle lift force. *J. Aerosol Sci.*4: 379-388.
10. Fan, B.J.; Wong, F.S.; McFarland, A.R.; Anand, N.K. (1992). Aerosol deposition in sampling probes. Accepted for publication in *Aerosol Sci. and Technol.*
11. Vincent, J.H.; Stevens; D.C.; Mark, D.; Marshall, M.; Smith, T.A. (1986). On the aspiration characteristics of large-diameter, thin-walled aerosol sampling probes at yaw orientations with respect to the wind. *J. Aerosol Sci.* 17:211-224.
12. Anand, N.K.; McFarland, A.R.; Kihm, K.D.; Wong, F.S. (1992). *Aerosol Sci. and Technol.* 16:105-112.
13. Friedlander, S.K.: Johnstone, H.F. (1957). Deposition of suspended particles from turbulent gas streams. *Ind. Eng. Chem.* 49: 1151-1156.
14. Davies, C.N. (1966). Deposition from moving aerosols. In: *Aerosol Science*. C.N. Davies, Ed. Academic Press, New York.
15. Onda, K. (1977). A review of theoretical and experimental studies of particle deposition in a turbulent flow. Memorandum Report 7, High Temperature Gasdynamics Laboratory, Mechanical Engineering Department, Stanford University, Palo Alto, CA.
16. Beal, S.K. (1970). Deposition of particles in turbulent flow on channel or pipe walls. *Nuclear Sci. and Eng.* 40: 1-11.
17. Pui, D.Y.H.; Romay-Novas, F; Liu, B.Y.H. (1987). Experimental study of particle deposition in bends of circular cross section. *Aerosol Science and Technol.* 7: 301-315
18. Cheng, Y.S.; Wang, C.S. (1975). Inertial deposition of particles in a bend. *J. Aerosol Sci.* 6: 139-145.
19. Tsai, C.J.; Pui, D.Y.H. (1990). Numerical study of particle deposition in bends of a circular cross-section — laminar flow regime. *Aerosol Sci. and Technol.* 12: 813-831.
20. Anand, N.K. and A.R. McFarland. (1991). DEPOSITION: Software to calculate particle penetration through aerosl transport lines. Office of Nuclear Regulatory Research, U.S. Nuclear Regulatory Commission, Washington, DC 20555. Draft Report for Comment, NUREG/GR-006.
21. McFarland, A.R.; Wong, F.S.; Anand, N.K.; Ortiz, C.A. (1991). Aerosol penetration through a model transport system: Comparison of theory and experiment. *Environ. Sci. & Technol.* 25:1573-1577.
22. Wong, F.S. (1992). Optimization of aerosol penetration through transport lines. M.S. Thesis. Department of Mechanical Engineering, Texas A&M University, College Station, TX 77843.
23. Strom, L. (1972). Transmission efficiency of aerosol sampling lines. *Atmos. Environ.* 6:133-142.
24. Glissmeyer, J.A.; Sehmel, G.A. (1991). Line-loss determination for air sampling systems. Office of Nuclear Reactor Regulation, U.S. Nuclear Regulatory Commission, Washington, DC 20555. NUREG/CR-4757.

DISCUSSION

DAVIS: Have you done testing at smaller particle sizes, below 0.5 μm, and how would they correlate with the larger particle sizes?

FAN: We have not conducted experiments with particles <0.5 μm diameter, but, the computer code does take into account losses caused by thermal diffusion of aerosol to the walls of straight tubes. These losses are predicted through the use of the sub-model of Beal, where Beal's equations have been shown by others to have good predictive ability.

FARAJIAN: Were experiments conducted to determine the limitations on the tube length for DOP testing in the nuclear industry?

FAN: No testing has been performed for the effect of the tube length on the sampling; however, since the basic depositional mechanisms are taken into account by the computer codes, we believe the code should be appropriate for use in predicting particle losses in long transport lines (50-70 m).

COSTIGAN: Does your code predict deposition of particles on individual components in the pipe system?

FAN: Yes, the code output can give particle losses of either monodisperse particles or particle distributions throughout the entire system.

HIGH EFFICIENCY AND ULTRA LOW PENETRATION AEROSOL FILTER TEST PROGRAMS BY THE EUROPEAN COMMUNITY COUNTRIES

R. G. Dorman

Consultant, Salisbury, SP1 3PX, UK
Convener, Working Group 2

Abstract

A short account is given of the deliberations of a CEN (European Standardization Committee) Working Group investigating new particulate test methods for HEPA/ULPA filters with a view to adoption of one as a European Standard.

I. Introduction

The European Document 4/4 for particulate testing of HEPA filters has existed for more than a decade; although not a mandatory test it has had wide usage. Based upon the sodium flame test developed in the United Kingdom and published as British Standard 3928:1969, it has undergone considerable improvement since that date, but with the advent of ULPA filters and modern particle counters came the desire to update the test or to replace it. The German Verband Deutscher Maschinen und Anlagenbau e V (VDMA) recommended that a group of experts should consider a new test. Their proposals were published in 1989 by the VDMA[1]. The test equipment designed to implement these proposals was to be housed in the Government Material Testing Institute (MPA NRW) in Dortmund[2].

II. Discussions and Programme

A meeting of a European Committee for Standardization, held in Brussels in 1989, was followed in 1990 by another, also in Brussels, which was attended by representatives from ten European countries. At this latter meeting Belgium was appointed as the country to hold the Secretariat of two working groups (WG1 and WG2) and, additionally, the Convenership of Working Group 1 while the United Kingdom took over the Convenership of Working Group 2 for HEPA and ULPA filter test methods. The purpose of this paper is with WG2 but it is worthwhile noting that WG1, concerned with general ventilation and air-conditioning filters has adopted the US ASHRAE test with little alteration. The choice of a test method has become more important recently with the drive towards unification of standards in Europe. Adoption of a European Standard will render national standards obsolete and could therefore involve test houses in considerable expense. For example, equipment might be too costly for the smaller manufacturer in capital outlay or in operational costs, forcing him to send all filters to a central test house. Another possibility might be to send only a proportion of HEPA and ULPA filters to be tested, but such a policy would obviously be unsatisfactory and has been fiercely attacked by several members of WG2.

At the 1990 Brussels meeting two methods of test were put forward. First, the UK sodium flame method with flame photometric

measurement of mass penetration, together with particle counting and sizing of the aerosol of sodium chloride generated from Dautrebande atomizers which provide particles mainly in the 0.01-0.4µm range. The second method, described by Mr R. Wepfer of Messrs LUWA, and supported by the German representatives, was essentially that proposed in the VDMA document already mentioned. In outline the steps are:-

(i) Measurement of the fractional efficiency as a function of particle size and pressure drop across a plane sheet of a filter medium at the envisaged operating velocity. The size for maximum penetration (MPPS) to be determined.

(ii) Testing of the filter element for leaks by scanning at the nominal test face velocity using a particle counting method with a neutralised aerosol of particles in a band around the MPPS as determined in (i). A condensation nucleus counter is employed in this test.

(iii) Testing of the performance of the filter, carried out in the same rig as in (ii) without removing the filter. Upstream measurement of concentration is made, if necessary with dilution equipment.

WG2 met at the premises of Messrs LUWA for a demonstration of the equipment. An aerosol of DES from a Rapaport-Weinstock generator was sized using a differential mobility analyser with 32 channels in the range 0.011 to 0.931 µm. Particles were found in 12 channels between 0.074 and 0.457 µm, approximately 36 per cent by number lying between 0.18 and 0.21 µm. A filter tested with this aerosol, assessing the penetration by condensation nucleus counter with scanning, gave a value of 0.00008 per cent, which was repeated in a further test. Each assessment took some 10 minutes.

At a subsequent meeting the UK presented results obtained on two filters by flame photometry of NaCl on a rig incorporating a particle counter. The aerosol was not neutralised and the particle counter/sizer (a helium-neon laser) was not especially calibrated for sodium chloride particles. No peak was found in the penetration curve, penetration in the nominally lowest channel of 0.1-0.15 µm being greater than in the 0.15-0.2 µm region. Somewhat crude calculations of mass penetrations from the particle penetration graph agreed within a factor of x2 with the mass penetration measured by flame photometry. The representative of the test house said that a more sensitive particle counter would be obtained.

The position at present is that members of the Working Group consider that test particles should be liquid, rather than solid, and that for filters of high efficiency scanning is a necessary part of the test. It was resolved at the fifth meeting in Vienna that ".... the principle of the Swiss/German method of test utilising a liquid test aerosol in the MPPS range with both upstream and downstream assessment is agreed. The method is accepted subject to obtaining satisfactory results from the new German rig and correlation with the

Swiss rig, together with an acceptable degree of repeatability. The method now to be adopted for the complete range of HEPA and ULPA filters."

A full report is expected to be given at the meeting to be held in Dortmund in September 1992.

If there is good correlation some simplification is likely to be necessary to speed the rate of test on the production line. Many members of the Working Group, while accepting the proposed method as a "Type Test" were concerned that, as demonstrated in Zurich, it was too slow for a production line. Their comments were incorporated in a previous Resolution laying down that ".... production line rigs and independent and accredited test houses should operate on the same principles but may utilise different standardized equipment and specified test procedures." Possible reduction in testing time might be achieved by reducing the number of channels to be counted. Consideration might also be given to an electrical aerosol analyser, while a laser sizer-counter has possibilities.

There is interest in methods being considered in the USA[3,4] and, although the range of WG2 discussion has so far been much less detailed than, for example, that of the IES (ref.3), there are grounds for expecting EEC and US test methods to be very similar.

Acknowledgements

This paper is presented with permission of CENTC/195

References

(1) Proposal for DIN-Standard, VDMA, Frankfurt (1989)

(2) Gross, H., New testing procedure for standard absolute (HEPA) and high performance absolute (ULPA filters, 10th International Symp. on Contam. Control, ICCCS, Zurich (1990)

(3) Testing of ULPA filters, IES-RP-CC-007-1.0 (Draft), Inst. Envir. Sci., (1991)

(4) Scripsick, R.C., and Soderholm, S.C., "Final report: Evaluation of methods, instrumentation, and materials pertinent to quality assurance filter penetration testing, LA-10748, UC-41, Los Alamos Nat. Lab., (1987)

THE EFFECTS OF TEMPERATURE ON HEPA FILTER MEDIA

C Hamblin and P J Goodchild
Separation Technology Department
AEA D&R Harwell
Oxon, England.

Abstract

This paper presents the results from a series of experiments to study the changes in the physical properties of HEPA filter media after exposure to elevated temperatures. Data are presented for papers heated in the range 120-500°C. The observed changes in strength and paper stiffness are explained in terms of alterations to the binder due to thermal degradation. The information generated has clarified a particular failure mode associated with a small number of filter inserts at elevated temperatures.

1 Introduction

A programme to assess the performance of high efficiency particulate air (HEPA) filters under hot dynamic conditions is well established at Harwell[1]. Recent tests, involving circular filter inserts have highlighted instances where the partial collapse of the pleats has led to insert failure after only 2-3 hours at temperatures of 200-300°C. Subsequent examinations have suggested this behaviour is strongly influenced by changes in the properties of the glass fibre based filtration media.

This report describes a series of experiments which clearly demonstrate that reductions in paper strength and rapid changes in stiffness result from modifications in binder structure. Increased understanding of these factors has allowed appropriate modifications to the relevant filter purchasing specifications which have substantially improved overall filter stability at elevated temperatures.

2 Experimental

2.1 Physical Tests

Testing was carried out on three proprietary grades of high efficiency filter papers comprising glass fibres of various lengths and diameters, and an organic binder to provide physical integrity. The papers (designated A, B and C) are regularly used in the HEPA filters supplied to the UK nuclear industry, and meet the performance criteria detailed in AESS 30/93400[2].

The paper manufacturing process can lead to significant variations in properties within a roll of medium. In order to minimise these effects, and to aid data analysis, sufficient specimens for a series of experiments were cut from localised areas of paper. Batches of specimens of the appropriate dimensions were

then heated at the test temperatures, in an air-purged furnace, for up to 500 hours. After cooling to ambient temperature, the following were measured:

(a) paper weight loss;
(b) tensile strength (machine direction (MD) values in accordance with BS 4415[3]);
(c) air burst resistance (in accordance with BS 6410[4]);
(d) Gurley stiffness values;
(e) dynamic stiffness (L'Homargy) values.

2.2 Changes in Binder Composition

Infra-red (IR) spectrographic and standard gravimetric analyses were employed to study general changes in binder composition during heating.

The method developed for the IR analysis involved refluxing 1 gramme samples of paper, for 4 hours, in 100ml of high purity acetone. 25ml aliquots of the acetone extracts were then evaporated to dryness, under a stream of nitrogen, and the residues re-dissolved in 1ml of acetone and re-evaporated with 400mg of potassium bromide. After grinding, 16mm diameter discs were pressed from the mixtures and IR spectra recorded over the range 4000-200cm^{-1}.

The total organic carbon (TOC) content of the papers was determined using a simple gravimetric technique. Samples were heated to 700°C in a stream of N_2/O_2, and the mass of CO_2 formed was determined after absorption in sodium hydroxide solution.

3 Results and Discussion

3.1 Binder Degradation

Early discussion of the changes in binder composition helps explain many of the paper test results summarised below.

Analysis of samples of the unheated papers showed 40-60% of each binder was acetone soluble, and their IR spectra to be closely related and consistent with acrylic polymer/co-polymer mixtures.

Sample weights were routinely measured, and Figure 1 illustrates typical media weight losses after 10 minutes at temperature. At temperatures below 400°C, weight losses were observed to increase when heating was continued beyond 10 minutes. For example, data summarised in Table 1 show weight loss to continue for up to 100 hours at 250°C. This appears to coincide with a progressive reduction in the amount of acetone soluble material present in each paper. The resulting IR spectra however, displayed similar (but weaker) absorbance bands to those obtained with acetone extracts from the unheated papers.

Table 1 also suggests significant amounts of binder remain after 500 hours at 250°C. This material, which was rapidly removed by heating at 450°C, may simply be the original acetone insoluble

components of the binders. It is more likely however, to be a mixture of thermally more stable (high carbon content) species formed during degradation reactions involving both acetone soluble and insoluble components. Although additional analytical methods are necessary to confirm this, it is clear that changes occur which may fundamentally alter the nature of the binders studied.

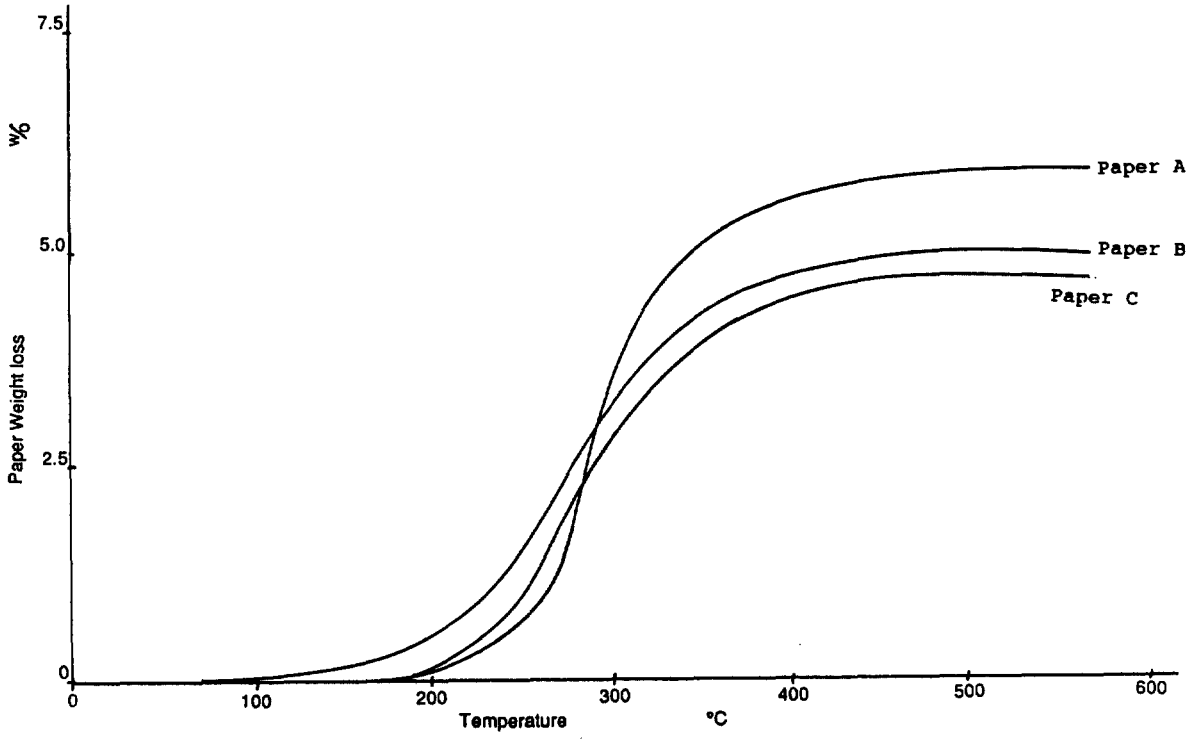

Figure 1 Typical Media Weight Loss Curves

Table 1: Typical Paper Weight Loss at 250°C

Time at 250°C (h)	Weight Loss (%)		
	A	B	C
0.2	0.6	1.0	0.8
1	0.7	1.3	1.3
5	2.3	2.1	1.6
10	3.9	2.9	2.3
25	4.4	3.3	2.5
50	4.7	3.6	2.6
100	4.8	3.8	2.7
500	4.8	3.9	2.7
Initial binder content of paper (%)	6.8	5.7	5.3

3.2 Paper Tensile Strength

The variation in paper tensile strength with temperature is illustrated in Figure 2. These data show that short term (10 mins) exposure to temperatures above 250°C results in reductions in paper strength which are directly linked to binder loss/ degradation.

After heating to 450°C, all three media have broadly similar trength properties (despite the initial strength advantage of paper). At this stage however, the papers are "binder free" and reliant on essentially similar glass fibres for their strength/ integrity.

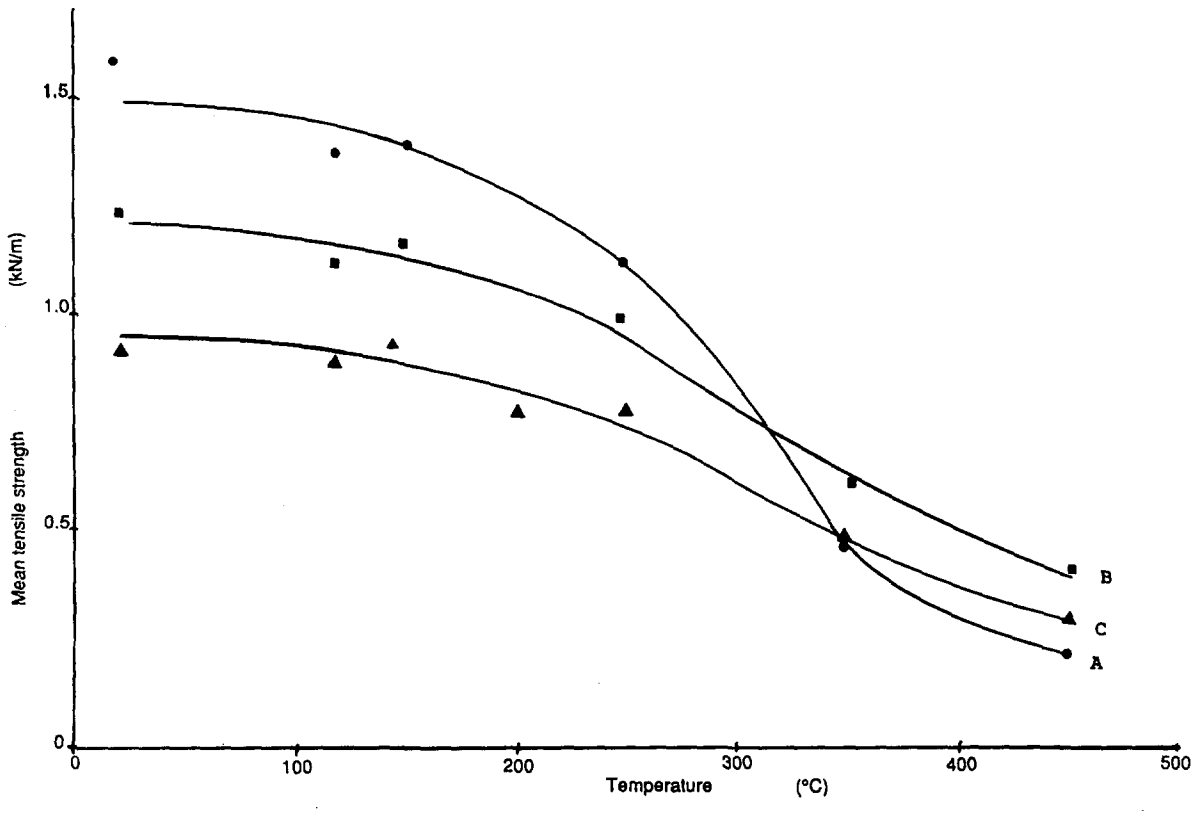

Figure 2 Effect of Temperature on Paper Tensile Strength

Table 2 also shows paper strength to be a function of time at temperature:

Table 2: Effect of Time At Temperature on Tensile Strength

Time at Temp (hours)	Mean MD Tensile strength (kN/m)								
	Paper A			Paper B			Paper C		
	120 °C	200 °C	250 °C	120 °C	200 °C	250 °C	120 °C	200 °C	250 °C
No heating	1.36	1.31	1.33	1.05	0.98	1.03	0.90	0.94	0.85
0.5	1.48	1.25	1.08	1.06	1.01	0.88	0.88	0.91	0.76
1	1.47	1.37	1.02	1.00	1.05	0.85	0.93	0.88	0.73
5	1.33	1.33	0.78	1.18	0.95	0.63	0.89	0.83	0.54
25	1.38	1.14	0.41	0.92	0.92	0.54	0.86	0.81	0.46
100	1.32	1.25	0.42	1.05	0.86	0.66	0.94	0.77	0.43
500	1.33	1.05	0.36	1.01	0.87	0.51	0.86	0.72	0.50
1000	1.45	1.14	0.38	1.05	0.71	0.47	0.88	0.76	0.44

Weight losses at temperatures below 200°C are small and, with the possible exception of Paper C, media strength is also unaffected at these temperatures. However, the changes in binder content/composition discussed above clearly influence paper strength at higher temperatures. Relatively rapid reductions in paper strength are observed at 250°C, with minimum values (0.3-0.5 kN/m) recorded after about 25 hours (in a similar manner to weight loss at this temperature). Although residual binder materials are still present at this stage, they appear to contribute little to the overall strength of the media.

3.3 Air Burst Resistance

Changes in air burst resistance follow similar trends to those observed for tensile strength, and representative data are summarised in Tables 3 and 4.

Table 3: Effect of Temperature on Paper Air Burst Resistance

Paper	Mean Air Burst Resistance (kPa)						
	Initial Value	120°C	150°C	200°C	250°C	350°C	500°C
A	11.5	11.0	11.7	10.8	9.3	4.0	4.1
B	9.1	9.3	9.0	8.8	8.3	4.5	4.3
C	8.6	9.0	8.0	8.4	8.0	4.3	4.3

Note: these results were obtained on samples heated for 10 minutes at the temperature indicated.

Table 4: Effect of Time at Temperature on Air Burst Resistance

Time at Temp (h)	Mean Air Burst Resistance (kPa)			
	Results Paper B		Results Paper C	
	120°C	250°C	120°C	250°C
0	8.8	9.2	7.8	8.1
1	8.3	8.1	8.5	7.4
10	7.9	8.3	7.3	4.7
50	7.8	4.1	6.8	3.8
100	8.9	3.8	7.5	5.2
500	7.5	4.2	7.9	3.9

3.4 Paper Stiffness

Correct paper stiffness is important in the production of circular filters. During the pleating process the medium is scored and folded by machine, and inappropriate paper stiffness can result in poorly defined pleats.

Gurley and L'Homargy stiffness measurements were made on media samples heated at 120°C, 200°C, 250°C and 350°C. Typical data are illustrated for papers A, B and C, in Figures 3, 4 and 5 respectively. Although additional work is necessary to fully quantify changes at 120°C, the data obtained clearly demonstrate heating results in initial increases in stiffness. The magnitude of these increases appear independent of temperature. The time at which maximum stiffness occurs (about 25 hours at 200°C, 2-3 hours at 250°C and 8-10 minutes at 350°C) is however, clearly influenced by temperature.

Changes in paper stiffness may also be related to the changes in the binder composition. The species formed during the initial degradation reactions, involving the acetone soluble fraction of the binders, increase media stiffness. As these species are themselves decomposed, stiffness is reduced to values below those recorded for unheated papers.

Clearly, these rapid changes in media stiffness and strength can influence pleat behaviour at elevated temperatures and contribute to filter failures. As a result, a minimum pleat strength requirement (of 0.5kN/m) has been included in the relevent filter purchasing specifications, and recent hot dynamic tests have shown significant improvements in filter performance at 200-300°C.

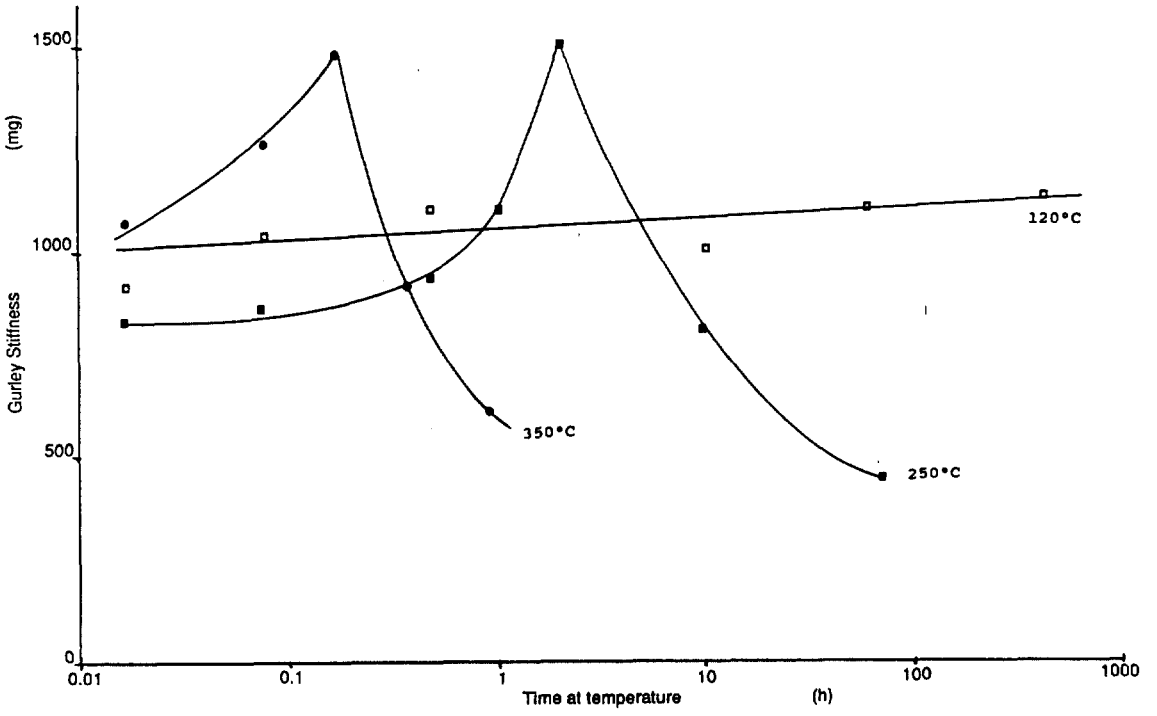

Figure 3 Effect of Temperature on Stiffness (Paper A)

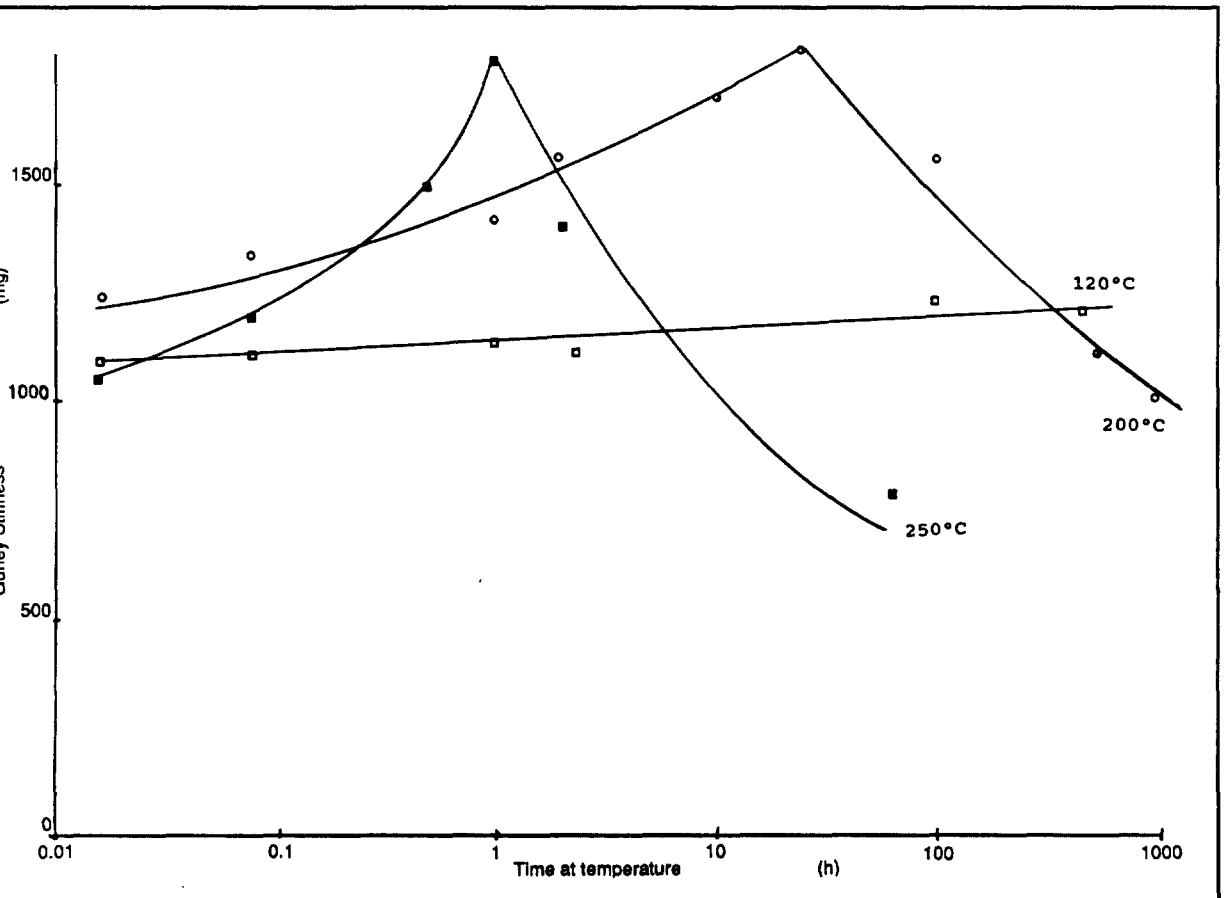

Figure 4 Effect of Temperature on Stiffness (Paper B)

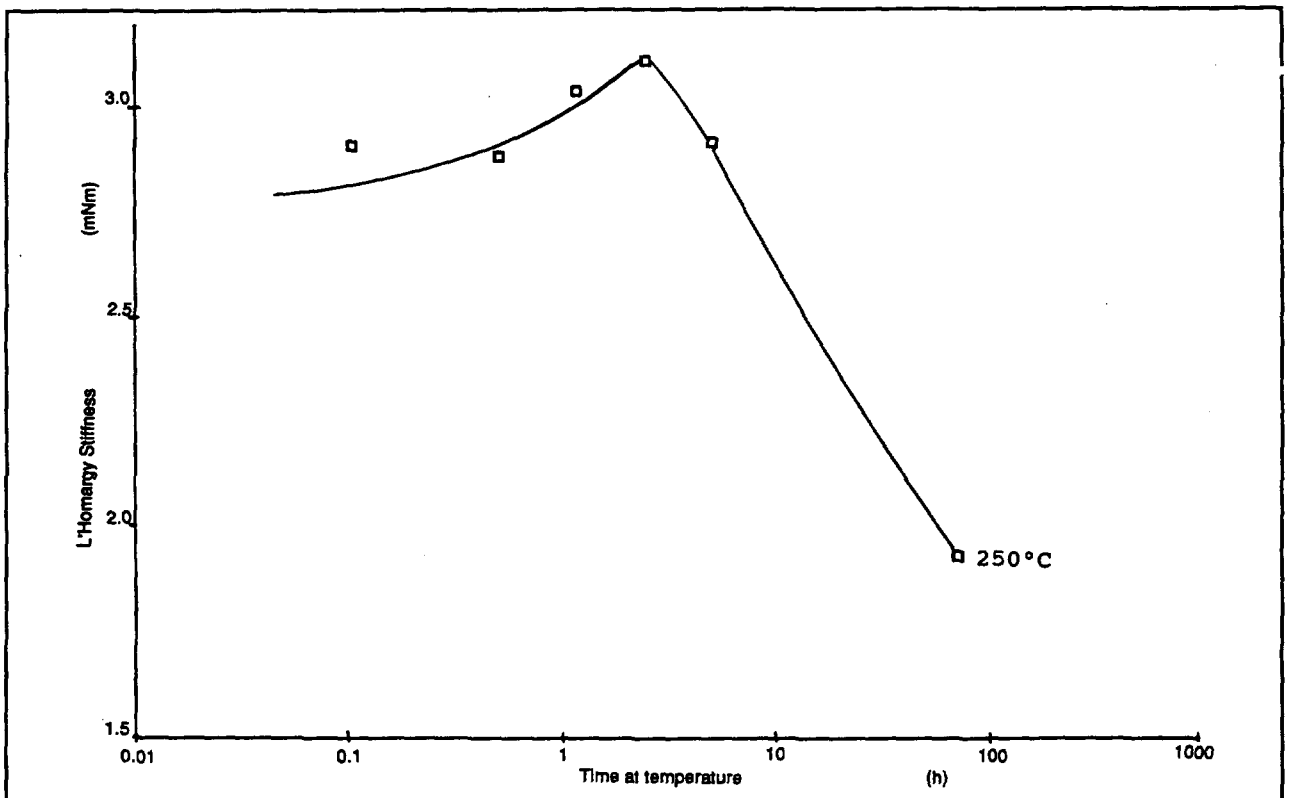

Figure 5 Effect of Temperature on Stiffness (Paper C)

6 Conclusions

- The properties of the glass fibre media used in these experiments were relatively unaffected by prolonged heating at 120°C.
- Exposures to temperatures above 120°C however, reduced both the tensile strength and air bust resistance of the papers used.
- The magnitude of the loss in strength is dependent on the temperature, and the time at temperature, and results from the degradation of the organic binders used in media production.
- Heating to 500°C leads to complete removal of the binder, and media strength are reduced to 0.3-0.5 kN/m at this stage.
- Media strength are also reduced to 0.3-0.5 kN/m after about 25 hours at 250°C. Binder materials are present at the stage, but they have little affect on paper strength.
- Heating glass fibre filtration media at 200-350°C results in initial increases in stiffness, which are reduced on further heating. The time at which maximum stiffness occurs is dependent on temperature and is also related to the changes in binder composition.

- The combination of increased paper stiffness and reduced strength may influence the stability of pleats at elevated temperatures, and contribute to filter failure.

Aknowledgement

This work was undertaken with financial support from the UK Department of Energy, which is now part of the UK Department of Trade and Industry, under the management of the Office of the Chief Technologist (Nuclear) of AEA Technology. The authors gratefully acknowledge this support and helpful advice from Dr J Williams of the Office of the Chief Technologist (Nuclear).

References

1. Pratt, R P and Stewart, B L. Performance testing of HEPA filters under hot dynamic conditions. 18th DOE Nuclear Air Cleaning Conf, 1984.

2. AESS 30/93400:1989, Filter medium for use in high efficiency particulate air (HEPA) filters/inserts.

3. BS 4415:1979, Method for the determination of tensile strength of paper and board.

4. BS 6410:1984, British standard methods of test for filter papers.

DISCUSSION

DAVIS: Are these binders generally acrylic based?

HAMBLIN: Yes, they are.

EDWARDS, J.: There is another observation that can be made with regard to loss of the binder at 500°C. The paper would have zero wet strength, or zero resistance to direct wetting, after loss of binder.

HAMBLIN: We did, in fact, observe this, but it is interesting to note that papers with a silicone-based water repellent retain their resistance to wetting after heating to 500°C.

CLOSING COMMENTS OF SESSION CO-CHAIRMAN MOELLER

Session 6 opened with a report from Germany on the installation of containment venting systems on their nuclear power plants, and the development of sampling systems to determine the post-accident status. To assure the collection of representative samples, in situ samplers have been developed that can be transported into containment. Related studies at Texas A&M University have led to the development of a computer code, DEPOSITION, that can be used to estimate aerosol losses through various sampling systems. Also reported were data on the performance of a commercial version of a new continuous air monitor for transuranic radionuclides that has been developed as a joint effort of the Los Alamos National Laboratory and Texas A&M University. One of the benefits of this monitor is its ability to eliminate the effects of airborne radon decay products.

The final portion of Session 6 was directed to filter performance and testing. Workers in the U.K. reported on the development of new particulate test methods for HEPA/ULPA filters, the goal being to establish one method as a European standard. The final paper in the Session summarized studies in the U.K. on the effects of temperature on HEPA filter media. This work showed that glass fiber filter media were relatively unaffected by prolonged heating at 120°C; however, exposures at higher temperatures reduced both tensile strength and air burst failure resistance.